SENSITIVITY ANALYSIS FOR NONLINEAR STRUCTURES

BY QIANG KONG

A dissertation submitted to the

Graduate School—New Brunswick

Rutgers, The State University of New Jersey

in partial fulfillment of the requirements

for the degree of

Doctor of Philosophy

Graduate Program in Mechanical and Aerospace Engineering

Written under the direction of

Professor Hae Chang Gea

and approved by

_____

_____

_____

_____

New Brunswick, New Jersey

January, 2008

ABSTRACT OF THE DISSERTATION

SENSITIVITY ANALYSIS FOR NONLINEAR STRUCTURES

by Qiang Kong

Dissertation Director: Professor Hae Chang Gea

Sensitivity analysis of total strain energy for nonlinear structures is studied. Based on the law of energy-consistent, the effective strain and stress have been defined to provide scalar measures of the strain and stress for the two and three dimensional problems. The total strain energy is transformed in the form of the effective stain and stress. A closed-form approach for sensitivity calculation is derived. This method can also be extended to large displacement, large rotation problems using the 2nd Piola-Kirchhoff stress and Green-Langrange stress.

The numerical examples with both geometric and material nonlinearity are presented to demonstrate the applications for the proposed sensitivity analysis calculation for strain energy. To evaluate the accuracy of the new method, numerical results obtained by the proposed method are compared with those from both analytical solution (for simple geometry) and finite differencing method.

The closed-form solution of design sensitivity is also applied for reliability-based structural design. Specifically, the case study is performed for the problem for the uncertain applied force performed, and uncertain Young's modulus with nonlinear materials. The numerical results obtained by the close-formed solution are compared with those from Monte Carlo simulation.

Acknowledgements

I would like to express my deepest appreciation to my advisor Prof. Hae Chang Gea for his valuable guidance and continuous encouragement throughout my doctoral studies. His friendly advice and high degree of motivation have been very helpful in my academic and personal aspects of my life.

I would also like to thank my committee members, Prof. Perumalsamy N. Balaguru, Prof. Assimina A. Pelegri, and Prof. Peng Song, for their interest in this research and for their valuable time in reviewing this dissertation. They have helped produce the best quality dissertation of my ability.

I wish to acknowledge my fellow graduate students and friends for their help and friendly company. In particular I wish to thank Jianhui Lou, Shangfu Zheng, Ching-Jui Chang, Euihark Lee, Po-Ting Lin and Wei-Ju Chen.

Support of this work by the Graduate School of Rutgers University, National Science Foundation and Center for the Computational Modeling of Aircraft Structures (CMAS) is deeply appreciated.

Dedication

To my daugher Fei-Fei

my wife Rui

Table of Contents

List of Tables

List of Figures

Chapter 1

INTRODUCTION

In general, optimization is concerned with achieving the best outcome of a given objective while satisfying certain restrictions. The motivation is to exploit the available limited resources in a manner that maximizes output or profit. The structural optimization is the research of design that is defined as " the rational establishment of a structural design that is the best of all possible designs within a prescribed objective and a given set of geometrical and/or behavioral limitations"(Olhoff and Taylor)[1].

The objective of this dissertation is to develop a systematic approach for design sensitivity analysis for non-linear structures.

One of the most challenging problems that has inhibited the application of structural optimization techniques to practical problems is the high computational cost required for such applications. The high cost is typically associated with the evaluation of constraint functions and their derivatives with respect to design variables. For many structural optimization problems, the evaluation of stress, displacement, or other behavioral constraint, requires the execution of costly finite element analyses. The optimization process may require evaluating constraint functions hundreds or thousands of times. The cost of repeating the finite element analysis so many times is usually prohibitive.

Design sensitivity analysis is the study of the determination of the rate of change with respect to a set of design parameters of one or more performance measures that are often expressed as functionals involving a combination of design and response fields. Sensitivity analysis plays an important role in; structural optimization, reliability analysis, inverse problems, and parameter identification problems. It can also be useful in guiding manual resign procedures. The central problem in sensitivity analysis is the determination of the implicit variations in the response fields generated by a specified design variation.

Due to an increasing demand for cost-efficient structures, computational methods

for Design Sensitivity Analysis and optimization have made considerable progress in the past decade. Most of the methods developed, however, are for linear systems. A general methodology that can handle nonlinear optimization problems does not exist although nonlinear structural analysis is a well-developed field. The development of optimization has been always limited to the linear elastic structures while the compliant devices undergo nonlinear deformation. When applying linear analysis based optimization to nonlinear designs, the final design often needs to be verified using a nonlinear analysis program(Nishiwaki, Min and Kikuchi, 1997). This approach carries an inherent defect: the optimality that was built upon a linear analysis program cannot survive on the nonlinear analysis. Therefore, the final design may satisfy the constraints, although it can be suspect, but it does not present itself as the optimal solution.

1.1 Classification of Nonlinear Analysis

Nonlinearity of structures can be classified as material nonlinearity and kinematic nonlinearity. Material nonlinearity is due to the nonlinear elastic and plastic behavior of the structural material. Kinematics nonlinearity occurs when the deflections are large enough to change the equations of equilibrium. Therefore, it is also called kinematic, or geometric nonlinearity. Table 1.1 gives a classification for different nonlinear effects - material nonlinear and kinematic nonlinear.

Figures 1, 2 and 3 each present an example of the types of problem as listed in Table 1.1. It shows that in a materially-nonlinear-only analysis, the nonlinear effect lies solely in the nonlinear stress-strain relation. The displacements and strains are infinitesimally small; therefore the usual engineering stress and strain measures can be employed in the response description. Considering the large displacements but small strain condition. We note that in essence the material is subjected to infinitesimally small strains measured in a body-attached coordinate frame x',y' while this frame undergoes large rigid body displacements and rotations. The stress-strain relation of the material can be linear or nonlinear.

As shown in Fig 1, 2 and 3 and Table 1.1, the most general analysis case is the one in which the material is subjected to large displacements and large strains. In this case the stress-strain relation is also usually nonlinear.

Type of analysis	Description	Stress and strain measure
Materially-nonlinear-only	Infinitesimal displacements and strains; the strain-strain relation is nonlinear	Engineering stress and strain
Large displacements, large rotations, but small strains	Displacements and rotations of fibers are large, but fiber extensions and angle changes between fibers are small; the stress-strain relation may be linear or nonlinear	Second Piola-Kirchhoff stress, Green-Lagrange strain Cauchy stress, Almansi strain
Large displacements, large rotations, and large strains	Fiber extensions and angle change between fibers are large, fiber displacements and rotations may also be large; the stress-strain relation may be linear or nonlinear	Second Piola-Kirchhoff stress, Green-Lagrange strain Cauchy stress, logarithmic strain

Table 1.1: **Classification of nonlinear analysis**

1.2 Review of Research in Sensitivity Analysis for Nonlinear Structures

In general, design sensitivity analysis and optimal design of structures have been classified in size design, shape design and topology design problems. In size design problems, the cross-sectional dimensions or stiffness of members are treated as design variables. In shape design problems, the configuration of the structure varies, so there are variable domain problems. In topology design, design variables are commonly related to the effective material properties.

Song(1986) used a simplified non-linear spring to study nonlinear elastic-plastic problems. Design sensitivity of global plate thickness of an elastic-plastic structural optimization problem was considered by Xu(1992) who carried out a direct differentiation with geometric stiffness matrix with respect to the size design variable. Shape optimization with geometric nonlinear continuum equations to obtain the first variation that was then used for sensitivity computation. There are also some other works that follow similar approaches for size and shape design variables, but a method that can be

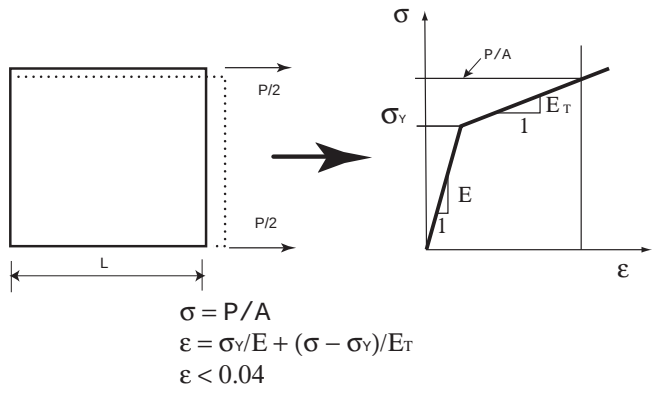

Figure 1.1: Materially-nonlinear (infinitesimal displacements, but nonlinear stress-strain relation

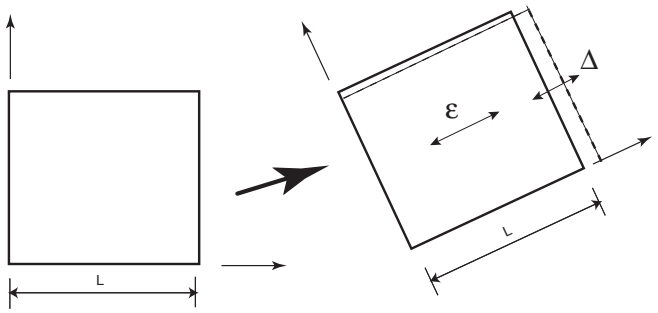

Figure 1.2: Large displacements and large rotations but small strains. Linear or nonlinear material behavior

directly used to solve nonlinear topology optimization has not yet been developed.

The theory of design sensitivity analysis in size design and shape design for nonlinear structural systems has been studied in recent years. The optimum design problem structure is one of the simplest problems that is formulated as a linear programming problem [1,2]. In the traditional approach, the material is idealized to be perfect plastic. Kaneko and Maier[3] discussed the optimum design problem of plastic structures with strain hardening. In their method, the optimum design problem is formulated as a quadratic programming problem and the solution is found using a criteria approach for optimization. Note that only a monotonic loading condition is considered in their work. Bendsoe and Sokolowski[4,5] presented a method of design sensitivity analysis and optimization of elastoplastic structures based on the analysis problem formulated as a quadratic programming problem. It is well recognized that Design Sensitivity Coefficients (DSC) of elastoplastic structures with linear kinematic hardening are not

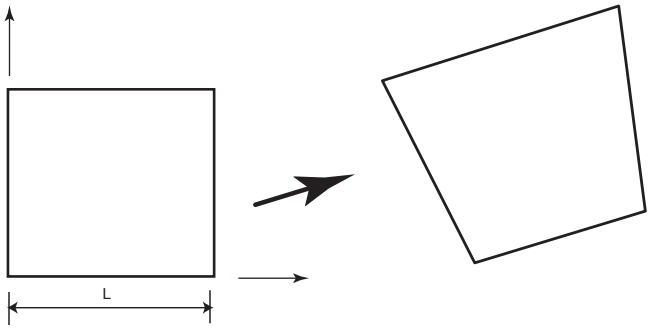

Figure 1.3: Large displacements, large rotations, and large strains. Linear or nonlinear material behavior

path-dependent when only the monotonic loading condition is considered. For example, DSCs do not depend on those at the previous incremental step. Therefore, DSCs can be found without resorting to any incremental procedure. Note that geometrical non-linearity cannot be taken into account in the methods presented in References 6 and 7. Since the analysis of structures with geometrical and material non-linearity should be carried out incrementally, DSA should also be an incremental procedure. Ray (et al.) presented a method for DSA of the dynamic response of frames with piecewise linear constitutive relations and without geometrical non-linearity. They pointed out that the time at which yielding occurs (yield time) in a member changes with design. DSCs of the yield time, however, were not calculated. Ray's method seems to be difficult to extend to DSA of distributed parameter structures with non-linear constitutive relations and with geometrical non-linearity. Tsay and Arora [8 .9] presented a general method for DSA for path-dependent problems. The application to specific problems and the difficulty due to the discontinuity of the DSC were discussed. Their method was successfully applied to an optimum design problem of an elastoplastic truss. However, implementation of the incremental form of DSA into an existing analysis code was not discussed. Mukherjee and Chandral presented a similar method based on the boundary element formulation. Recently, Arora and Lee and Lee et al. have discussed and verified the accuracy of the procedures using numerical examples. Vidal et al. have proposed an incremental method of DSA of path-dependent responses. It is noted in Reference 10 that a consistent tangent operator should be used to obtain accurate sensitivities. Their method has been successfully applied to a creep problem. Geometrical

non-linearity is not included in the formulation. The return mapping algorithm, which is necessary for elastoplastic problems, is not considered.

In general, there are four types of methods to solve nonlinear problem: the finite difference method, the adjoint variable method, the direct differentiation method[12] and the closed-form solution. Finite difference sensitivity analysis methods are simple to implement, but they can be computationally expensive and deficient in terms of accuracy and reliability[13,14]. For this reason, the adjoint variable and direct differentiation methods are generally preferred despite their relative complexity. One consequence of history-dependent behavior is that the response sensitivity at a given time and position depends on both the response and the response sensitivities at all previous times and locations in the structures. Reu et al. [13] were among the first to point this out. Incremental versions of the direct-differentiation method are natural choices for sensitivity analyses of history-dependent problems, since these methods generate sensitivity information for the complete response field at each step. Adjoint sensitivity formulations are not well-suited for step-by-step methods because each adjoint solution yields the sensitivity of only a single performance functional, rather than the sensitivities of the full response fields [14].

On the other hand, adjoint sensitivity analysis procedures involving a transient, terminal-value problem are feasible for a history-dependent problem. In this case, the sensitivity analysis can not be carried out simultaneously with the forward solution since the definition of the adjoint terminal-value problem depends on the solution of the original initial-value problem. This substantially increases the computational expense and complexity. Thus, the direct differentiation method is usually the method of choice for history-dependent problems.

The main challenge in formulating the direct differentiation method is the derivation of the incremental stress sensitivities as a function of the incremental response and total response sensitivities evaluated at the beginning of the time step. Several methods have been proposed over the past few years. Wu and Arora suggested that a semi-analytical approach could be used in combination with the differentiation method [15]. In this approach, the response sensitivities for analytical expressions that are difficult to derive are computed by the finite difference method. More recently, Tsay and co-worker [16,17] and Mukherjee and co-workers [18,19] have presented formulations of incremental

direct differentiation methods based on finite element and boundary element models. Mukherjee and co-workers used explicit methods to integrate the constitutive equations. This approach can be expensive since it requires the use of extremely small time steps to ensure accuracy. Tsay and co-workers present only analytical solutions and do not address the issue of numerical integration.

The main challenge of topology optimization for non-linear structures is the massive computational requirement of design sensitivity analysis. To reduce computational efforts, Taylor[20,21] presented a global extreme principle for softening and stiffening structures. Pedersen and Taylor[22] and Pedersen[23] presented a secant formulation using power-law model.

In this phase of evaluation, an attempt is made to determine the closed form solution of design sensitivity for strain energy for the materially nonlinear problems and the large displacement, large rotation but small strain problems. An effective strain and stress is defined under the law of energy-consistency and the relations between the effective strain and the effective stress are governed by a function which defines the nonlinearity of the problem. The representation of the strain energy of the structure can be transformed in the form of the effective strain and stress for sensitivity calculation. Following the conventional topology optimization formulation, design variables for the sensitivity calculation are chosen as volume fraction of "composite material" and a density function relating the design variable and material properties can be derived from the "composite material" model. Based on upon the "composite" model, the sensitivity analysis of strain energy for nonlinear structures is calculated. With this closed form solution for design sensitivity analysis, non-linear topology optimization can then be applied without excessive computational burden. Examples from simple power-law stress-strain relation are presented to validate the proposed approach. Numerical examples of other nonlinear structures compared with those from the finite difference method are also presented.

1.3 Research Contributions

The main contribution of this dissertation is the development of a generalized and exact solution of sensitivity analysis for nonlinear structures. The main achievements are as follows:

- *Modeling of nonlinear elasticity*

  Based upon the law of energy-consistency, a scalar form of the effective strain for nonlinear structures is defined and its corresponding effective stress is derived from the energy-consistent relation.

- *Study of sensitivity analysis for total strain energy for nonlinear structures*

  The closed form solutions of the total strain energy has been derived and verified based on the modeling of nonlinear structures. The solution is extended to the geometric nonlinearity.

- *Study of application of structural reliability based optimization design*

  The closed-form solution of design sensitivity of structural reliability is derived by the effective models defined from the energy consistent point of view.

1.4 The Chapters Ahead

In Chapter 2, a equivalent effective model is proposed to model nonlinear structures. A scalar form of the effective strain for nonlinear structures is defined and its corresponding effective stress is derived from an energy-consistent relation first. This model can also be extended to geometric nonlinearity.

Chapter 3 deals with closed-form solution for sensitivity analysis of total strain energy for nonlinear structures with generalized nonlinear material behaviors. With this closed form solution for design sensitivity analysis, nonlinear topology optimization can be applied without excessive computational burden. In this chapter, numerical examples are presented to demonstrate the application for the proposed sensitivity analysis calculation for strain energy.

In Chapter 4, a generalized closed form solution of sensitivity analysis for structures with nonlinearity is used to study the sensitivity of strain energy for end-loaded, large deflection beams. To verify the accuracy of sensitivity calculation by effective strain based method, in this chapter, the expressions of sensitivity of total strain energy will derived by both the classical approach and proposed method.

Chapter 5 extends the effective strain based sensitivity analysis to reliability design. The goal of the chapter is to derive a closed-form solution of design sensitivity of

structural reliability. That is, we want to deal with sensitivity for reliability-based design problems by effective models from an energy consistent point of view.

Chapter 6 extends the modeling of non-linear elasticity to nonlinear hyper-elasticity. In this study, the closed-form solution has been derived for sensitivity of total strain energy for nonlinear hyper-elasticity. Several numerical examples are presented to verify the results.

Chapter 7 is focused on the study of sensitivity of strain energy with uncertain variables. In the chapter, both cases of uncertain applied force and uncertain Young's modulus are studied. Numerical examples are again presented to verify the results.

Finally in Chapter 8, a brief conclusion and discussion are presented, and further extension of the current work is proposed.

Chapter 2

Modeling of nonlinear elasticity

2.1 Introduction

In contrast to the situation with linear systems, out of the various area of interest in structural optimization relatively little is available in the form of general results for constitute nonlinear systems. A most notable exception to this is the extensive set of classical work done in the area of optimal design relative to plastic collapse, dated mostly from the decade starting in the mid-1950(the name Prager, Shield, and Drucker figure prominently in this subject; Martin (1975) provides a comprehensive overview of the research of the era). Developments from this period were based on the specific model of a perfectly plastic solid material working in an isotropic and homogeneous system.(Modeling for structural optimization in fact reflects design for maximum collapse load). At the same time, clearly on practical grounds it would be useful to have a better understanding of analysis and design for more general nonlinear materials. This is justified most simply on the basis that the behavior of most ordinary engineering materials is distinctly nonlinear. Clearly, knowledge of the means to predict optimal structural design in the face of material degradation nonlinearity would have immediate technical application as well.

As a step in the direction toward development of effective means for the treatment of constitutive nonlinear problems, we present results from a study of analysis and design related to a more general form of nonlinear material. Bell (1972) provides much information on the use since antiquity of this still common material models identified there as 'Exponential Law'. His earliest citation is to work of James Bernoulli done in 1694! Relatively more contemporary applications of power law type models are given in Ramberg & Osgood(1943), Tvergaard (1983), and Ju and Kyriakides(1991). The relation between this sort of modeling and reality is empirical, i.e., something realized essentially through curve-fitting, and it is a convenient form for such application. The

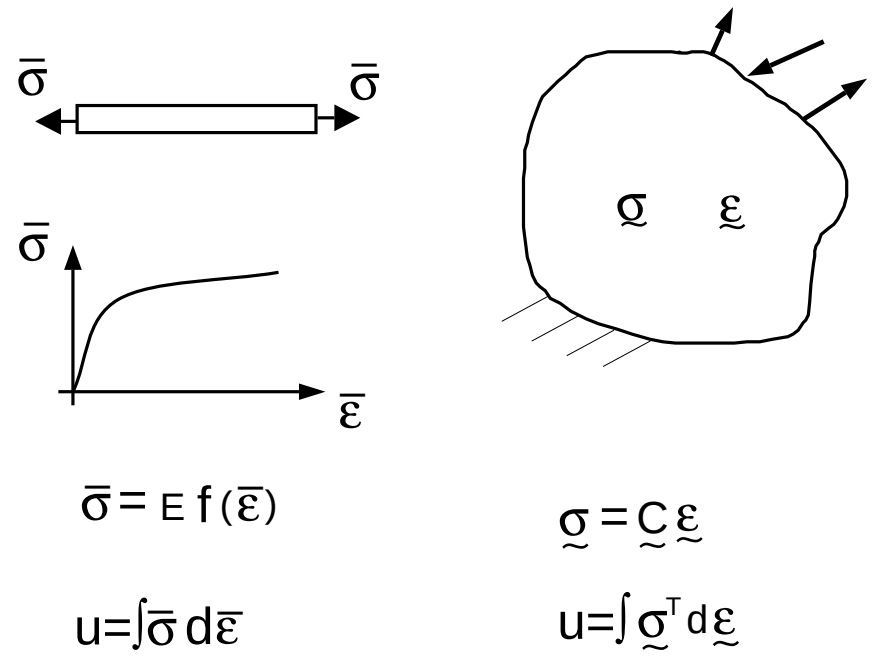

Figure 2.1: Modeling for nonlinear elasticity

work reported here is centered on the power law model because the simplicity in its form provides conveniently for the kind of development undertaken in our study.

In this chapter, a number of independent, general results are obtained in connection with the modeling for optimal design of structures made of generalized form nonlinear behavior. In addition, the expression for energy densities associated this material are discussed, and a useful relation between strain energy density and complementary strain energy density is observed. The chapter also provides for the evaluation of the design derivative of total strain energy in terms of local derivatives(sensitivities). These results are extended in next section to define the problem for geometric non-linearity.

2.2 Constitutive matrices modeled by effective strains

For the two and three dimensional problems, we also need a scalar measure of the strain(or stress) state, termed the effective strain. To be specific let us first show the formulation in terms of strains.

The effective strain is defined in the form of strains as

$$\bar{\varepsilon}^2 = \boldsymbol{\varepsilon}^T \boldsymbol{C_0} \boldsymbol{\varepsilon} \tag{2.1}$$

where ε is the strain state and $\boldsymbol{C_0}$ is a symmetric, positive definite and dimension-less

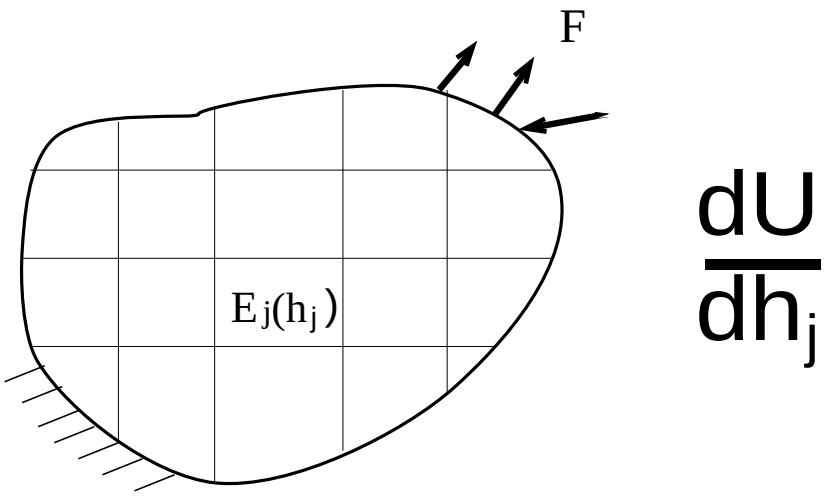

Figure 2.2: Discrete structure

matrix. For isotropic materials, it can be expressed in terms of Poisson's ratio as

$$\boldsymbol{C_0} = \frac{1-\nu}{(1+\nu)(1-2\nu)} \begin{bmatrix} 1 & \frac{\nu}{1-\nu} & \frac{\nu}{1-\nu} & 0 & 0 & 0 \\ \frac{\nu}{1-\nu} & 1 & \frac{\nu}{1-\nu} & 0 & 0 & 0 \\ \frac{\nu}{1-\nu} & \frac{\nu}{1-\nu} & 1 & 0 & 0 & 0 \\ 0 & 0 & 0 & \frac{1-2\nu}{2(1-\nu)} & 0 & 0 \\ 0 & 0 & 0 & 0 & \frac{1-2\nu}{2(1-\nu)} & 0 \\ 0 & 0 & 0 & 0 & 0 & \frac{1-2\nu}{2(1-\nu)} \end{bmatrix} \tag{2.2}$$

From the energy-consistent point of view, the strain energy density, u, should be a consistent either derived from the effective strain and stress, $\overline{\varepsilon}$ and $\overline{\sigma}$, or from the structure strain and stress strain, ε and σ. Therefore, the following relation must hold,

$$u = \int \boldsymbol{\sigma}^T d\boldsymbol{\varepsilon} = \int \overline{\sigma} d\overline{\varepsilon} \tag{2.3}$$

Hereby, the effective stress is implicitly defined from Eq (2.3). Taking a total differential for Eq (2.1) leads to

$$\overline{\varepsilon} d\overline{\varepsilon} = \boldsymbol{\varepsilon}^T \boldsymbol{C_0} d\boldsymbol{\varepsilon} \tag{2.4}$$

combining Eq (2.3) and Eq (2.4), and noting the relation stated in Eq (2.3) remains true for any strain state. The constitutive relation between the structure stress and strain can be expressed as

$$\boldsymbol{\sigma} = \frac{\overline{\sigma}}{\overline{\varepsilon}} \boldsymbol{C_0} \boldsymbol{\varepsilon} \tag{2.5}$$

By pre-multiplying $\boldsymbol{\sigma}^T \boldsymbol{C_0}^{-1}$ to both sides of Eq (2.5) and utilizing the definition from Eq (2.1), the effective stress can be expressed directly as

$$\overline{\sigma}^2 = \boldsymbol{\sigma}^T \boldsymbol{C_0}^{-1} \boldsymbol{\sigma} \tag{2.6}$$

This result agrees with the known definition of effective stress(Pedersen and Taylor 1993). Similar to Eq (2.4), a total differential to Eq (2.6) gives

$$\boldsymbol{\sigma}^T \boldsymbol{C_0}^{-1} d\boldsymbol{\sigma} = \overline{\sigma} d\overline{\sigma} \tag{2.7}$$

From Eq (2.5), we also can get

$$\boldsymbol{\varepsilon}^T = \frac{\overline{\varepsilon}}{\overline{\sigma}} \boldsymbol{\sigma}^T \boldsymbol{C_0}^{-1} \tag{2.8}$$

Considering the stress energy density u^c of the structure is defined as

$$u^c = \int \boldsymbol{\varepsilon} d\boldsymbol{\sigma} \tag{2.9}$$

Inserting Eq (2.7) and Eq (2.8), Eq (2.9) becomes

$$\begin{aligned} u^c &= \int \frac{\overline{\varepsilon}}{\overline{\sigma}} \boldsymbol{\sigma}^T \boldsymbol{C_0}^{-1} d\boldsymbol{\sigma} \\ &= \int \overline{\varepsilon} d\overline{\sigma} \end{aligned} \tag{2.10}$$

It is clear to see that the resulting relation agrees with our prior derivations in strain energy.

2.3 Strain energy density, stress energy density and work equations

The relation between effective stress/strain and structure stress/strain can be correlated from work equation. The work done by the external force can be obtained from

$$\begin{aligned} w &= u + u^c \\ &= \boldsymbol{\sigma}^T \boldsymbol{\varepsilon} \end{aligned} \tag{2.11}$$

Substituting Eq (2.1) and Eq (2.5) in Eq (2.11), we have,

$$\begin{aligned} w &= \frac{\overline{\sigma}}{\overline{\varepsilon}} \boldsymbol{\varepsilon}^T \boldsymbol{C_0} \boldsymbol{\varepsilon} \\ &= \overline{\sigma}\, \overline{\varepsilon} \end{aligned} \tag{2.12}$$

Eq (2.12) simplifies to the work equation for a simple uniaxial tension problem represented by the effective stress and strain.

Generally, the nonlinear stress may be an arbitrary function of the strain, i.e,

$$\overline{\sigma} = E f(\overline{\varepsilon}) \tag{2.13}$$

where E is the modulus for a reference state. Clearly, $f(\overline{\varepsilon})$ should be a increasing function with respect to $\overline{\varepsilon}$. By substituting Eq (2.13) in Eq (2.3), Eq (2.5) and Eq (2.12), the strain energy density, the stress energy density and the virtual work are expressed as

$$\begin{aligned} u &= E\int f(\overline{\varepsilon})d\overline{\varepsilon} \\ u^c &= \int E\overline{\varepsilon}f'(\overline{\varepsilon})d\overline{\varepsilon} \\ w &= E\overline{\varepsilon}f(\overline{\varepsilon}) \end{aligned} \tag{2.14}$$

where $f'(\overline{\varepsilon}) = df(\overline{\varepsilon})/d\overline{\varepsilon}$.

For special case, when $f(\overline{\varepsilon}) = \overline{\varepsilon}^n$, inserting it to Eq (2.14), we obtain

$$\begin{aligned} u &= \frac{E}{n+1}\overline{\varepsilon}^{n+1} \\ u^c &= \frac{nE}{n+1}\overline{\varepsilon}^{n+1} \\ w &= E\overline{\varepsilon}^{n+1} \end{aligned} \tag{2.15}$$

It can be seen that Eq (2.15) is reduced to the following known results for nonlinear elasticity modeled by power-law stress-strain relation:

$$\begin{aligned} u^c &= nu \\ w &= (n+1)u \end{aligned} \tag{2.16}$$

2.4 Explicit relation between effective strains and real strains

For uniaxial problems, we know

$$\varepsilon_z = -\nu\varepsilon_x, \varepsilon_y = -\nu\varepsilon_x \tag{2.17}$$

By substituting Eq (2.17) in Eq (2.1) and Eq (2.5), we obtain,

$$\overline{\varepsilon}^2 == {\varepsilon_x}^2 \tag{2.18}$$

$$\sigma_x = \overline{\sigma} \tag{2.19}$$

We can observe that effective stress and strain are the same as real effective stress and strain for one-dimensional problems

For plane stress problems, we have

$$\varepsilon_z = -\frac{\nu}{(1-\nu)}(\varepsilon_x + \varepsilon_y) \tag{2.20}$$

By substituting in Eq (2.1)and Eq (2.5), we obtain the relation between effective stresses/strains and effective stresses/strains,

$$\overline{\varepsilon}^2 = \frac{1}{1-\nu^2}[\varepsilon_x^2 + {\varepsilon_y}^2 + 2\nu\varepsilon_x\varepsilon_y + \frac{1-\nu}{2}\gamma_{xy}^2] \tag{2.21}$$

$$\sigma_x = \frac{\overline{\sigma}}{\overline{\varepsilon}}\frac{\varepsilon_x + \nu\varepsilon_y}{(1-\nu)(1+\nu)} \tag{2.22}$$

$$\sigma_y = \frac{\overline{\sigma}}{\overline{\varepsilon}}\frac{\varepsilon_y + \nu\varepsilon_x}{(1-\nu)(1+\nu)} \tag{2.23}$$

$$\sigma_{xy} = \frac{\overline{\sigma}}{\overline{\varepsilon}}\frac{1}{1+\nu}\gamma_{xy} \tag{2.24}$$

We also obtain the relations for 3-D solid

$$\overline{\varepsilon}^2 = \frac{1}{(1-2\nu)(1+\nu)}[(1-\nu)(\varepsilon_h^2+\varepsilon_y^2+\varepsilon_z^2)+2\nu(\varepsilon_h\varepsilon_y+\varepsilon_y\varepsilon_z+\varepsilon_z\varepsilon_h)+\frac{(1-2\nu)}{2}(\gamma_{xy}^2+\gamma_{yz}^2+\gamma_{zx}^2)] \tag{2.25}$$

$$\sigma_x = \frac{\overline{\sigma}}{\overline{\varepsilon}}\frac{(1-\nu)\varepsilon_h + \nu(\varepsilon_y+\varepsilon_z)}{(1-2\nu)(1+\nu)} \tag{2.26}$$

$$\sigma_y = \frac{\overline{\sigma}}{\overline{\varepsilon}}\frac{(1-\nu)\varepsilon_y + \nu(\varepsilon_h+\varepsilon_z)}{(1-2\nu)(1+\nu)} \tag{2.27}$$

$$\sigma_z = \frac{\overline{\sigma}}{\overline{\varepsilon}}\frac{(1-\nu)\varepsilon_z + \nu(\varepsilon_y+\varepsilon_h)}{(1-2\nu)(1+\nu)} \tag{2.28}$$

$$\sigma_{xy} = \frac{\overline{\sigma}}{\overline{\varepsilon}}\frac{1}{1+\nu}\gamma_{xy} \tag{2.29}$$

$$\sigma_{xz} = \frac{\overline{\sigma}}{\overline{\varepsilon}}\frac{1}{1+\nu}\gamma_{xz} \tag{2.30}$$

$$\sigma_{yz} = \frac{\overline{\sigma}}{\overline{\varepsilon}}\frac{1}{1+\nu}\gamma_{yz} \tag{2.31}$$

2.5 Modeling for geometric nonlinearity

The geometric nonlinearity occurs when the deflections are large enough to cause significant changes in the geometry of the structure, such that the equations of equilibrium must be formulated for the deformed configuration.

Let dS and ds denote the length of a line element in reference and current configuration, respectively. The lagrangian strain tensor $\boldsymbol{S}$ and its Cartesian components E_{ij} are then defined by

$$ds^2 - dS^2 = 2d\boldsymbol{X}\boldsymbol{E}\boldsymbol{X} = 2E_{ij}dX_i dX_j \tag{2.32}$$

For a rigid-body motion the difference $ds^2 - dS^2$ is equal to zero. The components of $\boldsymbol{E}$ must in that case be equal to zero, and $\boldsymbol{E}$ is thus an objective tensor.

The Lagrangian strain tensor can be expressed in terms of the deformation gradient tensor $\boldsymbol{H}$ as

$$\begin{aligned} \boldsymbol{E} &= \frac{1}{2}(\boldsymbol{H^T H} - \boldsymbol{I}) \\ E_{ij} &= \frac{1}{2}(\frac{\partial x_k}{\partial X_i}\frac{x_k}{X_j} - \delta_{ij}) \end{aligned} \tag{2.33}$$

The second Piola-Kirchhoff stress tensor $\boldsymbol{E}$ can be also shown to be an objective tensor. It is related to the true, Cauchy stress tensor $\boldsymbol{\sigma}$ by

$$\begin{aligned} \boldsymbol{S} &= \frac{\nu^0}{\nu}(\boldsymbol{H^{-1}})\boldsymbol{\sigma}(\boldsymbol{H^{-1}})^T \\ S_{ij} &= \frac{\nu^0}{\nu}\frac{\partial X_i}{\partial x_k}\partial X_j \sigma_{kl} \partial X_j \partial x_l \end{aligned} \tag{2.34}$$

where ν and ν_0 are mass densities in current and reference configuration, respectively

Noticing the relation between the reference position vector $\boldsymbol{X}$, the current position vector $\boldsymbol{x}$, and the displacement vector $\boldsymbol{u}$,

$$\begin{aligned} \boldsymbol{x} &= \boldsymbol{X} + \boldsymbol{u} \\ x_i &= X_i + u_i \end{aligned} \tag{2.35}$$

we can express the Lagrangian strain components E_{ij} in terms of displacement gradients as

$$E_{ij} = \frac{1}{2}(u_{i,j} + u_{j,i}) + \frac{1}{2}(u_{k,i}u_{k.j}) = \varepsilon_{ij} + \theta_{ij} \tag{2.36}$$

where the comma denotes differentiation with respect to reference coordinates, and ε_{ij} is the linear Lagrangian or engineering strain tensor.

Consider now a small part of a continuum in a fixed Cartesian coordinate system $X_i, i = 1, 2, 3$, with base vectors I_i. If you apply a finite rotation, defined by the orthogonal rotation tensor $\boldsymbol{R}$. Note that a vector $d\boldsymbol{X}$ turns into a new vector $d\boldsymbol{X^*}$, where $d\boldsymbol{X^*} = \boldsymbol{R}d\boldsymbol{X}$ and $|d\boldsymbol{X}| = |d\boldsymbol{X^*} = dS$. Furthermore, $X_i^*, i = 1, 2, 3$, can be another Cartesian coordinate system with base vectors I_i, that is initially coinciding with X_i, but rotating with the body.

Now, give the body an infinitesimal deformation so that the vector $d\boldsymbol{X^*}$ turns into $d\boldsymbol{X}$. The vector $d\boldsymbol{X}$ has the component forms $d\boldsymbol{X} = dx_i I_i = dx_i^* I_i^*$. We, furthermore, have the relation form $d\boldsymbol{X} + d\boldsymbol{u} = d\boldsymbol{X^*} + d\boldsymbol{u}$, where $d\boldsymbol{u}$ is the relative displacement vector between two neighboring particles.

Let's see what occurs when $|d\boldsymbol{X}| = d\boldsymbol{s}$. The difference $ds^2 - dS^2$ can thus, in view of Eq (2.32), be written as:

$$\begin{aligned} ds^2 - dS^2 &= 2d\boldsymbol{X}d\boldsymbol{E}d\boldsymbol{X} = 2E_{ij}dX_i dX_j \\ &= 2d\boldsymbol{X^*}d\boldsymbol{E^*}d\boldsymbol{X^*} = 2E^*_{ij}dX^*_i dX^*_j \end{aligned} \tag{2.37}$$

It should be emphasized that the displacement gradient du_i/dX_j is of finite magnitude, while $du^*_i/dX^*_j << 1$. This implies that the quadratic part of the strain tensor E^*_{ij} can be neglected, and we can write $dX_i = dx_i$. We find that $E_{ij} = Eij^*$, and finally

$$E_{ij} = \varepsilon^*_{ij} \tag{2.38}$$

In other words, in case of small strains, but large deformations, the Lagrangian strain tensor components are equal to the engineering strain components in a system rigid-body rotating with the practice.

According to the polar decomposition theorem, the deformation gradient tensor $\boldsymbol{F}$ can be multiplicicatively decomposed into a rotation tensor $\boldsymbol{R}$ and a stretch tensor $\boldsymbol{U}$ as

$$\boldsymbol{F} = \boldsymbol{RU} \tag{2.39}$$

For infinitesimal strain the stretch tensor can be expressed as

$$\boldsymbol{U} = \boldsymbol{I} + \varepsilon\boldsymbol{A} \tag{2.40}$$

where ε is a small number and $\boldsymbol{A} : \boldsymbol{A} = \boldsymbol{II}$ The deformation gradient can thus be approximated by

$$\boldsymbol{F} = \boldsymbol{R} \tag{2.41}$$

Noting that $\nu_0/\nu = 1$ in the case of infinitesimal strain, we can express the second Poila-Kirchhoff stress tensor as

$$\boldsymbol{S} = (\boldsymbol{F^{-1}})^T\boldsymbol{\sigma}(\boldsymbol{F^{-1}}) = \boldsymbol{R\sigma R^T} \tag{2.42}$$

The component forms of the Cauchy stress tensor $\boldsymbol{\sigma}$ are $\boldsymbol{\sigma} = \sigma_{ij}I_iI_j = \boldsymbol{\sigma^*_{ij}}I^*_iI^*_j$, when I^*_i is a base vector in the previously introduced co-rotating Cartesian coordinate system.

The matrices of tensor components σ_{ij} and σ^*_{ij} are thus related by

$$[\boldsymbol{\sigma}] = [\boldsymbol{R}]^T[\boldsymbol{\sigma^*}][\boldsymbol{R}] \tag{2.43}$$

with $[\boldsymbol{R}]$ as the matrix of the components of $\boldsymbol{R}$ in the fixed system.

Combing Eq (2.42) and Eq (2.43), we finally get

$$[\boldsymbol{S}] = [\boldsymbol{R}([\boldsymbol{R}]^T[\boldsymbol{\sigma^*}][\boldsymbol{R}])[\boldsymbol{R}]^T = [\boldsymbol{\sigma^*}] \tag{2.44}$$

This result can be interpreted in case of small strain, the second Piola-Kirchhoff stress components are equal to the Cauchy stress components in a system rigid-body rotating with the particle.

The important conclusion one can draw from the above discussion is that a constitutive relation, formulated for the case of infinitesimal strain and rotation, and relating Cauchy stress and engineering strain or rates of these quantities, can be used unaltered to related Lagrangian strain and second Piola-Kirchhoff stress.

The constitutive relation is expressed in terms of second Piola-Kirchoff stress tensor and Lagrangian strain tensor as

$$\boldsymbol{S} = \boldsymbol{C_n}\boldsymbol{\epsilon} \tag{2.45}$$

when $\boldsymbol{C_n}$ is constitutive tangent matrix, $\boldsymbol{S}$ is the second Piola-Kirchoff stress tensor, $\boldsymbol{\epsilon}$ is and the Lagrangian finite strain tensor:

$$E_{ij} = \frac{1}{2}(\frac{\partial u_i}{\partial X_j} + \frac{\partial u_j}{\partial X_i} + \frac{\partial u_k}{\partial X_i}\frac{\partial u_k}{\partial X_j}) \tag{2.46}$$

where u_i denotes displacement.

We recognize that in infinitesimal displacement analysis, the relation of Eq (2.45) is reduced to the description used in general small deformation analysis because under these conditions the stress and strain variables reduces to the engineering stress and strain measures. However, an important observation is that in large displacement and large rotation but small strain analysis, the relation in Eq (2.45) provides a natural material description because the components of the second Piola-Kirchoff stress and Lagrangian strain tensors do not change under rigid rotation(Bathe 1996). Thus, only the actual straining of material will yield an increase in the components of the stress tensor. As long as this material straining(accompanied by large rotations and displacements) is small, the use of the relation in the Eq (2.45) is completely equivalent to the constitutive relation in infinitesimal displacement conditions. $\boldsymbol{C_n}$ depends only on the material properties for large deformation with small strain problems.

Similarly, for large deformation with small strain problems, the effective strain is also defined as

$$\bar{\varepsilon}^2 = \boldsymbol{\epsilon}^T \boldsymbol{C_0} \boldsymbol{\epsilon} \tag{2.47}$$

where $\boldsymbol{C_0}$ has the same meaning as material nonlinearity. Constitutive matrices modeled by the effective strain can be thus completely used in the formulation of large deformation cases.

Chapter 3

Sensitivity Analysis for Energy in Non-linear material Nonlinearity

3.1 Introduction

Sensitivity analysis of strain energy involves a calculation of the variation in the strain energy response with respect to the design variables. Following the conventional topology optimization formulation, design variables for the sensitivity calculation are chosen as a volume fraction of "composite material" and a density function relating to the design variable. Material properties can be derived from the "composite material" model. In this section, the sensitivity analysis of strain energy for nonlinear structures is calculated based on the effective nonlinear elastic model discussed in chapter 2.

3.2 Sensitivity analysis for generalized material nonlinearity

Sensitivity for strain energy is defined as

$$\frac{dU(\varepsilon(h),h)}{dh} \tag{3.1}$$

where h is the design field, and U is the total strain energy. The total strain energy is defined as:

$$U = \int u dV \tag{3.2}$$

where u is the strain energy density. From the analysis in chapter 2, for generalized nonlinear materials, the relation between effective stress and strain is expressed as

$$\overline{\sigma} = E(h) f(\overline{\varepsilon}(h)) \tag{3.3}$$

where E is the modulus and only dependent on design variables, and f is a function of the effective strain. The strain energy density can thus be written as

$$u = E(h) \int f(\overline{\varepsilon}) d\overline{\varepsilon} \tag{3.4}$$

Differentiating the total strain energy with respect to the design variable, sensitivity can be written as

$$\begin{aligned}\frac{dU}{dh} &= \int_V \frac{du}{dh} dV \\ &= \int_V [(\frac{\partial u(\overline{\varepsilon}(h),h)}{\partial h})|_{\overline{\varepsilon}} + (\frac{\partial u(\overline{\varepsilon}(h),h)}{\partial \overline{\varepsilon}(h)})(\frac{\partial \overline{\varepsilon}(h)}{\partial h})|_h] dV \\ &= \int [\int f(\overline{\varepsilon}) d\overline{\varepsilon} \frac{\partial E}{\partial h} + E(h) f(\overline{\varepsilon}(h))(\frac{\partial \overline{\varepsilon}(h)}{\partial h})] dV \end{aligned} \tag{3.5}$$

From Eq (3.5) , a closed-form solution for the sensitivity calculation becomes a discovery for the explicit expression of $\partial\overline{\varepsilon}(h)/\partial h$.

Let's begin with the work equation for a dead load system in terms of effective strain and stress, which was derived in chapter 2.

$$w = \overline{\sigma}\,\overline{\varepsilon} \tag{3.6}$$

By substituting Eq (3.3) in Eq (3.6), we can get

$$w = E(h)\overline{\varepsilon}(h) f(\overline{\varepsilon}(h)) \tag{3.7}$$

Differentiating Eq (3.7) with respect to design parameter h, one obtains

$$\frac{dw}{dh} = \overline{\varepsilon} f(\overline{\varepsilon}) \frac{\partial E}{\partial h} + E(f(\overline{\varepsilon}) + \overline{\varepsilon} f'(\overline{\varepsilon})) \frac{\partial \overline{\varepsilon}}{\partial h} \tag{3.8}$$

Let's look at the left side of Eq (3.8), which may be written in greater detail by means of

$$\frac{dw}{dh} = \frac{\partial w}{\partial h} + \frac{\partial w}{\partial \varepsilon} \frac{\partial \varepsilon}{\partial h} \tag{3.9}$$

where ε represents the strain field in total. The principles of virtual work, that hold for solid structures in equilibrium are

$$\frac{\partial w}{\partial \varepsilon} = \frac{\partial u}{\partial \varepsilon} \tag{3.10}$$

For design-independent loads

$$\frac{\partial w}{\partial h} = 0 \tag{3.11}$$

By inserting Eq (3.10) and Eq (3.11) and recognizing that $\overline{\varepsilon}$ is the only variable of the function of ε, Eq (3.9) simplifies to

$$\frac{dw}{dh} = \frac{\partial u}{\partial \overline{\varepsilon}} \frac{\partial \overline{\varepsilon}}{\partial h} = E f(\overline{\varepsilon}) \frac{\partial \overline{\varepsilon}}{\partial h} \tag{3.12}$$

By substituting Eq (3.12) in Eq (3.8), we get

$$Ef(\overline{\varepsilon})\frac{\partial\overline{\varepsilon}}{\partial h} = \overline{\varepsilon}f(\overline{\varepsilon})\frac{\partial E}{\partial h} + E(f(\overline{\varepsilon}) + \overline{\varepsilon}f'(\overline{\varepsilon}))\frac{\partial\overline{\varepsilon}}{\partial h} \tag{3.13}$$

A reorganization of Eq (3.13) results in:

$$\frac{\partial\overline{\varepsilon}(h)}{\partial h} = -\frac{f(\overline{\varepsilon}(h))}{E(h)}\frac{\frac{\partial E(h)}{\partial h}}{\frac{\partial f(\overline{\varepsilon}(h))}{\partial\overline{\varepsilon}(h)}} \tag{3.14}$$

Finally, the closed-form solution, in terms of effective strains, can be obtained by substituting Eq (3.14) in the expression of design sensitivity, Eq (3.5),

$$\begin{aligned}\frac{dU}{dh} &= \int_V [\int_{\overline{\varepsilon}} f(\overline{\varepsilon}(h))d\overline{\varepsilon}\frac{\partial E(h)}{\partial h} - \frac{f^2(\overline{\varepsilon}(h))}{\frac{df(\overline{\varepsilon}(h))}{d\overline{\varepsilon}}}\frac{\partial E(h)}{\partial h}]dV \\ &= \{\int_V [\int_{\overline{\varepsilon}} f(\overline{\varepsilon}(h))d\overline{\varepsilon} - \frac{f^2(\overline{\varepsilon}(h))}{f'(\overline{\varepsilon}(h))}]dV\}\frac{\partial E(h)}{\partial h}\end{aligned} \tag{3.15}$$

3.2.1 Linear and power-law elasticity

To verify this closed-form solution, let's consider the sensitivity analysis of minimum-compliance design for linear elastic materials and nonlinear elastic materials modeled by the power-law stress-strain relation.

For linear elasticity

$$f(\overline{\varepsilon}) = \overline{\varepsilon} \tag{3.16}$$

By substituting it in the Eq (3.15),

$$\frac{dU}{dh} = \int_V (\frac{\overline{\varepsilon}^2}{2} - \overline{\varepsilon}^2)dV\frac{\partial E}{\partial h} \tag{3.17}$$

and reorganizing it, we get

$$\frac{dU}{dh} = -\int_V \frac{\overline{\varepsilon}^2}{2}dV\frac{\partial E}{\partial h} = -(\frac{\partial U}{\partial h})|_{\overline{\varepsilon}} \tag{3.18}$$

It can be seen from Eq (3.18) that Eq (3.15) is reduced to the known result for linear elasticity (Pedersen 1991)

Similarly, for nonlinear elasticity, modeled by the power-law stress-strain relation of

$$f(\overline{\varepsilon}) = \overline{\varepsilon}^n \tag{3.19}$$

and substituting Eq (3.19) in the Eq (3.15),

$$\frac{dU}{dh} = \int_V (\int_{\overline{\varepsilon}} \overline{\varepsilon}^n d\overline{\varepsilon} - \frac{\overline{\varepsilon}^{2n}}{n\overline{\varepsilon}^{n-1}})dV\frac{\partial E}{\partial h} \tag{3.20}$$

after reorganizing it, we obtain

$$\frac{dU}{dh} = -\frac{1}{n}\int_V \frac{\overline{\varepsilon}^{n+1}}{n+1} dV \frac{\partial E}{\partial h} \tag{3.21}$$

So, our result also matches the known result(Pedersen 1991),

$$\frac{dU}{dh} = -\frac{1}{n}(\frac{\partial U}{\partial h})|_{\overline{\varepsilon}} \tag{3.22}$$

3.2.2 Localized sensitivity

When design variable h_i is a local design variable, related to design domain i, strain energy outside this domain is changing and thus one would expect an accumulative determination of dU/dh_i to be necessary.

Total strain energy is written as the sum of the domain strain energies, i.e.:

$$U = \sum_{i=1}^{N} \int_{V_i} E_i \int_{\overline{\varepsilon}} f(\overline{\varepsilon}) d\overline{\varepsilon} dV_i \tag{3.23}$$

where E_i, V_i are modulus and the volume of the i-th domain. N is the number of domains.

From Eq (3.15), the sensitivity of total strain energy to local change can be derived as :

$$\frac{dU}{dh_i} = [\int_{V_i} (\int f d\overline{\varepsilon} - \frac{f^2}{f'}) dV_i] \frac{\partial E_i}{\partial h_i} \tag{3.24}$$

3.3 Numerical results

In this section, a 2-D and a 3-D numerical example with both geometric and material nonlinearity are presented to demonstrate the application for the proposed method in sensitivity analysis.

MSC/NASTRAN commercial finite element codes for geometric nonlinearity are used to obtain standard structural analysis results.

To evaluate the accuracy of the new method, numerical results obtained by the proposed method are compared with those from a finite difference derivative, whereas the design sensitivity is expressed as $\Delta U/\Delta h$. For each example, we assume the material modulus is a function of design variables. For example,

$$E_i = E_{i0} g(h) \tag{3.25}$$

where E_{i0} is modulus constant of i-th element,

$$g(h) = h^2 \qquad \text{with} \;\; 0 \leq h \leq 1 \tag{3.26}$$

The following three different material behaviors are studied for each example:

Case 1: The softening material modeled by the power-law stress-strain relation,

$$f(\overline{\varepsilon}) = \overline{\varepsilon}^n \qquad \text{with} \;\; n < 1. \tag{3.27}$$

The stress-strain behavior is shown in Figure 1.

Case 2: The hardening material modeled by the power-law stress-strain relation,

$$f(\overline{\varepsilon}) = \overline{\varepsilon}^n \qquad \text{with} \;\; n > 1. \tag{3.28}$$

The stress-strain behavior is shown in Figure 2.

Case 3: For typical rubber-like material behavior, stress-strain relation can be described in the following form of a series expansion

$$f(\overline{\varepsilon}) = \overline{\varepsilon} - 40\overline{\varepsilon}^2 + 625\overline{\varepsilon}^3. \tag{3.29}$$

The stress-strain behavior is shown in Figure 3.

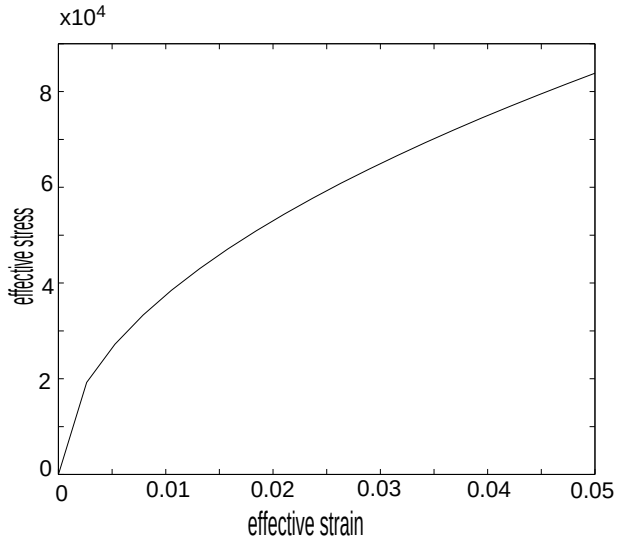

Figure 3.1: The stress-strain behavior: case 1(power law with $n < 1$)

3.3.1 Solution Algorithm

For the given nonlinear stress-strain relation presented in the curve along with material property as Yong's modulus and the Poisson's ratio, the computation procedures is described below:

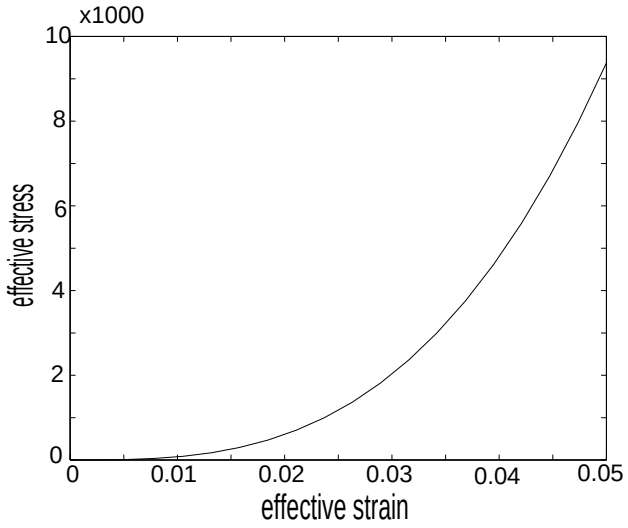

Figure 3.2: The stress-strain behavior: case 2(power law with $n > 1$)

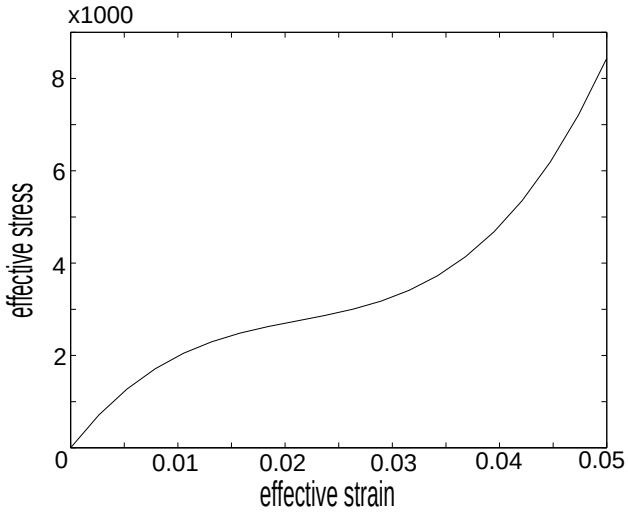

Figure 3.3: The stress-strain behavior: case 3(typical rubber behavior)

Step 1. Input values: $\{\sigma\}_{old}$, $\{\varepsilon\}_{old}$, $\{\Delta\varepsilon\}$, E, ν

Step 2. Calculate the new strain as

$$\{\varepsilon\}_{new} = \{\varepsilon\}_{old} + \{\Delta\varepsilon\} \tag{3.30}$$

Step 3. The effective strain ($\overline{\varepsilon}$) is computed based on $\{\varepsilon\}_{new}$ by

$$\overline{\varepsilon}^2 = \frac{1}{E} < \varepsilon > \{\sigma_e\} \tag{3.31}$$

where

$$\{\sigma_e\} = [D_e]\{\varepsilon\} \tag{3.32}$$

or

$$\overline{\varepsilon} = \frac{1}{1-\nu^2}[\varepsilon_x^2 + \varepsilon_y^2 + 2\nu\varepsilon_x\varepsilon_y + \frac{1-\nu}{2}\gamma_{xy}^2] \qquad \text{for plane stress} \tag{3.33}$$

$$\overline{\varepsilon} = \frac{1}{(1-2\nu)(1+\nu)}[(1-\nu)(\varepsilon_x^2+\varepsilon_y^2+\varepsilon_x^2)+2\nu(\varepsilon_x\varepsilon_y+\varepsilon_x\varepsilon_x+\varepsilon_y\varepsilon_z)+\frac{1-2\nu}{2}(\gamma_{xy}^2+\gamma_{xz}^2+\gamma_{yz}^2)] \qquad \text{for 3-D} \tag{3.34}$$

Step 4. The effective stress ($\overline{\sigma}$) is determined by looking-up the stress-strain curve for $\overline{\varepsilon}$

Step 5. The new stress state is determined by

$$\overline{\sigma}_{new} = \frac{\overline{\sigma}}{E\overline{\varepsilon}}\{\sigma_e\} \tag{3.35}$$

Step 6. The tangential matrix is determined by

$$[D_{ne}] = \frac{\overline{\sigma}}{E\overline{\varepsilon}}[D_e] + \frac{1}{(E\overline{\varepsilon})^2}(\frac{\partial\overline{\sigma}}{\partial\overline{\varepsilon}} - \frac{\overline{\sigma}}{\overline{\varepsilon}})\{\sigma_e\}\{\sigma_e\}^T \tag{3.36}$$

for which $\frac{\partial\overline{\sigma}}{\partial\overline{\varepsilon}}$ is the slope at $\overline{\varepsilon}$,

$$\frac{\partial\overline{\sigma}}{\partial\overline{\varepsilon}} = \frac{y_{k+1} - y_k}{x_{k+1} - x_k} \tag{3.37}$$

where (x_k, y_k) is the k-th data point for the strain-strain curve and k is determined such that $x_k \leq \overline{\varepsilon} \leq x_{k+1}$. It is noted that $k = 1$ for $\overline{\varepsilon} \leq x_1$ and $k = k_{max} - 1$ for

$$\overline{\varepsilon} \geq x_{max}$$

3.3.2 Adaptation of Uniaxial Compression Stress-Strain Curve

Since some materials exhibit appreciably different behaviors in compression from that in tension even in the small strain range, the uniaxial compression data can not be ignored.

For uniaxial loading, the magnitude of the strain in that direction becomes the effective strain.

$$\overline{\varepsilon} = \varepsilon_x \qquad \text{for uniaxiable tension in } x \tag{3.38}$$

$$\overline{\varepsilon} = -\varepsilon_x \qquad \text{for uniaxiable compression in } x \tag{3.39}$$

We need to find the effective stress ($\overline{\sigma}$) corresponding to $\overline{\varepsilon}$. There are two known data points, namely the effective stress for uniaxial tension ($\overline{\sigma}_t$) and the effective stress for uniaxial compression ($\overline{\sigma}_c$). The method of interpolation or extrapolation is required to predict the effective stress for the general stress state using two known data points.

The first stress invariant (I_1) is adopted for interpolation/extrapolation.

$$I_1 = \overline{\sigma}_x + \overline{\sigma}_y + \overline{\sigma}_z \tag{3.40}$$

Considering that the pure shear is in the midway between simple tension and simple compression, it seems appropriate to use the first stress invariant. Hydrostatic tension and compression cases will impose the lower and upper bounds for extrapolation.

$$I_1 = \sigma_x \qquad \text{for uniaxiable tension/compression} \tag{3.41}$$

$$I_1 = 0 \qquad \text{for pure shear} \tag{3.42}$$

$$I_1 = 3p \qquad \text{for hydrostatic pressure} \tag{3.43}$$

The instantaneous modulus ($\frac{\partial \overline{\varepsilon}}{\partial \overline{\varepsilon}}$) should be interpolated or extrapolated in the same manner.

3.3.3 Computational Procedure for Bilateral Stress-Strain Relations

The new stress state is proportional in magnitude to the effective stress ($\overline{\sigma}$), which should be determined as follows:

1. Compute the effective stress ($\overline{\sigma}_e$) based on $\{\overline{\sigma}_e\}$, i.e.,

$$\{\sigma_e\} = [D_e]\{\varepsilon\}_{new} \tag{3.44}$$

$$\overline{\sigma} = \sqrt{\frac{1}{2}[(\sigma_x - \sigma_y)^2 + (\sigma_y - \sigma_z)^2 + (\sigma_x - \sigma_x)^2] + 3(\tau_{xy}^2 + \tau_{yz}^2 + \tau_{zx}^2)} \quad \text{for 3D} \tag{3.45}$$

$$\overline{\sigma} = \sqrt{\sigma_x^2 - \sigma_x\sigma_y + \sigma_y^2 + 3\tau_{xy}^2} \quad \text{for plane stress} \tag{3.46}$$

$$\overline{\sigma} = \sqrt{\frac{1}{2}[(\sigma_x - \sigma_y)^2 + (\sigma_y - \sigma_z)^2 + (\sigma_x - \sigma_x)^2] + 3\tau_{xy}^2} \quad \text{for plane strain} \tag{3.47}$$

2. Compute the first invariant of $\{\sigma_e\}$:

$$I_1 = \overline{\sigma}_x + \overline{\sigma}_y + \overline{\sigma}_z \tag{3.48}$$

where $\sigma_z = 0$ for plane stress.

3. Determine the ratio (r) by normalizing I_1 by $\overline{\sigma}_e$,

$$r = \frac{I_1}{\overline{\sigma}_e} \tag{3.49}$$

where r signifies the relative distance from the midpoint of $\overline{\sigma}_c$ and $\overline{\sigma}_t$ at $\overline{\varepsilon}$. It would be implausible to process with a large value of r (such is the case with a hydrostatic load). Therefore, r will be confined to a plausible range, $-1 \leq r \leq 1$. The value will be reset to the limit $r = \pm 1$ if r lies outside the range.

4. Look up the effective stress-strain curve and determine $\overline{\sigma}_t$ and $\overline{\sigma}_c$.

$$\overline{\sigma}_t = \overline{\sigma}(\overline{\varepsilon}) \tag{3.50}$$

$$\overline{\sigma}_t = -\overline{\sigma}(-\overline{\varepsilon}) \tag{3.51}$$

No. of elem	New method	Finite difference derivative	The relative difference
1	-44.2424	-44.7733	1.2%
5	-17.3095	- 17.5864	1.6%
10	-25.3461	-25.8277	1.9%
15	-30.1345	-30.5865	1.5%

Table 3.1: **Comparison of the results of plane for case 1**

5. Determine $\overline{\sigma}$ based on $\overline{\sigma}_t$, $\overline{\sigma}_c$, and r.

$$\overline{\sigma} = \frac{\overline{\sigma}_t + \overline{\sigma}_c}{2} + r\frac{\overline{\sigma}_t - \overline{\sigma}_c}{2} \tag{3.52}$$

For the tangent matrix, the instantaneous modulus $(\frac{\partial\overline{\sigma}}{\partial\overline{\varepsilon}})$ should be determined using the same ratio (r) as follows:

a) Compute the instantaneous slope at $\overline{\varepsilon}$ for tension.

$$(\frac{\partial\overline{\sigma}}{\partial\overline{\varepsilon}})_t = \frac{y_{i+1} - y_i}{x_{i+1} - x_i} \qquad \text{for } x_i \le \overline{\varepsilon} \le x_{i+1} \tag{3.53}$$

where (x_i, y_i) is the i-th data point in the effective stress-strain curve.

b) Compute the instantaneous slop at $-\overline{\varepsilon}$ for compression.

$$(\frac{\partial\overline{\sigma}}{\partial\overline{\varepsilon}})_c = \frac{y_{j+1} - y_j}{x_{j+1} - x_j} \qquad \text{for} x_j \le -\overline{\varepsilon} \le x_{j+1} \tag{3.54}$$

c) Determine $(\frac{\partial\overline{\sigma}}{\partial\overline{\varepsilon}})$ based on $(\frac{\partial\overline{\sigma}}{\partial\overline{\varepsilon}})_t$, $(\frac{\partial\overline{\sigma}}{\partial\overline{\varepsilon}})_c$, and r.

$$\frac{\partial\overline{\sigma}}{\partial\overline{\varepsilon}} = \frac{1}{2}[(\frac{\partial\overline{\sigma}}{\partial\overline{\varepsilon}})_t + (\frac{\partial\overline{\sigma}}{\partial\overline{\varepsilon}})_c] + \frac{r}{2}[(\frac{\partial\overline{\sigma}}{\partial\overline{\varepsilon}})_t - (\frac{\partial\overline{\sigma}}{\partial\overline{\varepsilon}})_c] \tag{3.55}$$

3.3.4 Example 1: two-dimensional plane

A simple two-dimensional plane is considered as a first example to study the application and accuracy of the proposed approach. This example has 3×15 finite elements and external loads that are applied to the free end of beam(Figure 3). The results in Tables 1, 2 and 3, represent the sensitivities of total strain energy of four different elements calculated by the new method and finite difference derivative method, as well as their relative differences for nonlinear material behaviors of cases 1, 2 and 3 respectively. As shown in Tables 1, 2 and 3, sensitivity predictions are in close agreement with finite difference results for three different material behaviors with large deformation.

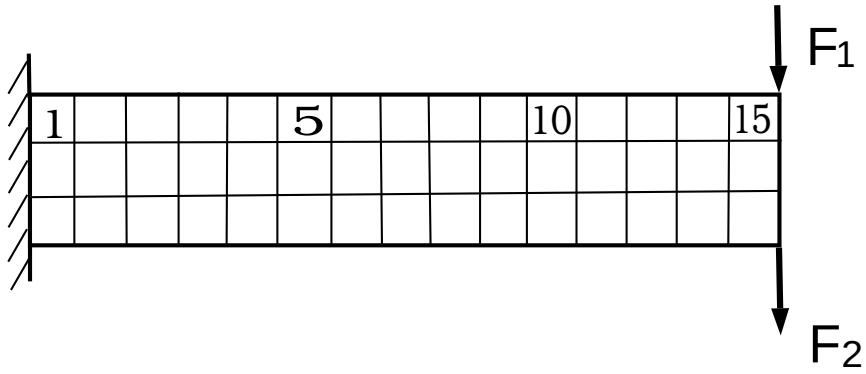

Figure 3.4: Example 1: two dimensional plane

No. of elem	New method	Finite difference derivative	The relative difference
1	-8.0211	-8.0932	0.9%
5	-3.4509	-3.4854	1.0%
10	-4.8777	-4.9460	1.4%
15	-7.3111	-7.4207	1.5%

Table 3.2: **Comparison of the results of plane for case 2**

No. of elem	New method	Finite difference derivative	The relative difference
1	-7.2314	-7.2892	0.8%
5	-3.4987	-3.5442	1.3%
10	-4.5423	-4.6013	1.3%
15	-6.3409	-6.4170	1.2%

Table 3.3: **Comparison of the results of plane for case 3**

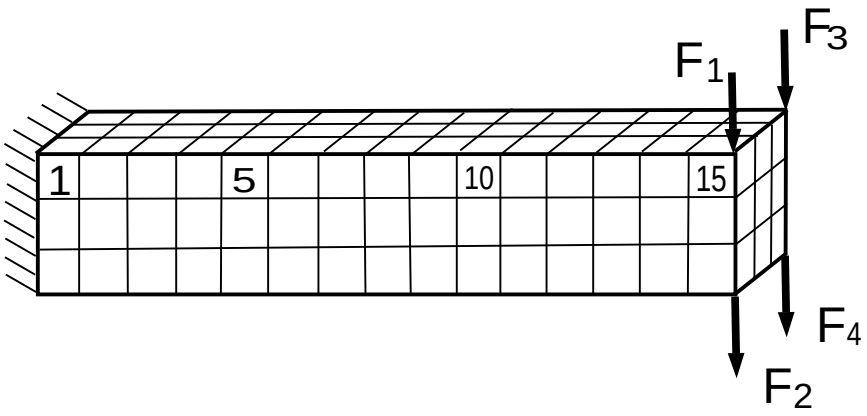

Figure 3.5: Example 2: 3-D solid

No. of elem	New method	Finite difference derivative	The relative difference
1	-10.0098	-10.2400	2.3%
5	-5.8861	-6.0921	3.5%
10	-6.6541	-6.7805	1.9%
15	-7.2311	-7.3757	2.0%

Table 3.4: **Comparison of the results of 3-D solid for case 1**

3.3.5 Example 2: 3-D solid

The second example presents a 3-D problem with $3 \times 3 \times 15$ finite elements as external loads are applied to the free end of beam(Figure 4).

The results in Tables 4, 5 and 6 represent the sensitivities of four different elements for a 3-D solid obtained by the new method and finite different derivative method, as well as their relative differences for cases 1, 2 and 3 nonlinear material behaviors respectively. As shown in Table 4, 5 and 6, excellent agreement exists between sensitivity prediction obtained from proposed method and finite differences that is obtained for three dimensional model.

No. of elem	New method	Finite difference derivative	The relative difference
1	-30.9982	-31.5252	1.7%
5	-10.2322	-10.5392	3.0%
10	-17.2154	-17.5941	2.2%
15	-22.6600	-23.1359	2.1%

Table 3.5: **Comparison of the results of 3-D solid for case 2**

No. of elem	New method	Finite difference derivative	The relative difference
1	-27.2398	-27.8118	2.1%
5	-10.0982	-13.6326	3.5%
10	-15.2321	-15.6434	2.7%
15	-20.3327	-20.8003	2.3%

Table 3.6: **Comparison of the results of 3-D solid for case 3**

Chapter 4

Sensitivity Analysis for Geometric Nonlinearity

4.1 Introduction

The geometrically non-linear analysis and design of mechanical structures and components is of importance in practical applications because there are a number of important applications where large flexibility and deflection are desirable and necessary for the system to function. The compliant mechanism is such an example. Since compliant mechanisms depends on deflection for their motion, the deflections are often large, resulting in geometric non-linearities. A considerable amount of work has been done in non-linear mechanics to characterize the deflections of flexible beams(Bisshopp and Drucker, 1945; Frisch-Fay, 1962; Gorski, 1976), but much remains to be done in light of the applications introduced by the recent development of compliant mechanism theory.

There are several methods for sensitivity analysis that take into account the nonlinearities introduced by large deflection. A classical method is based on the direct differentiation for deflection equation(Mattiasson, 1981; Howell and Leonard 1998). An advantage of this method is that it provides closed-form solutions, but the derivatives are cumbersome and solutions exist for only relatively simple geometries and loadings. General design sensitivity analysis of nonlinear structures is studied by Aurora and his co-workers(1985, 1990a, 1990b). Shape sensitivity analysis of non-linear structures has been developed by Choi(1987 and 1992). However, the efficient method for sensitivity analysis for topology design has not yet been developed.

In the chapter 1, a generalized closed form solution of design sensitivity for strain energy was derived. This method is based on the law of energy-consistency and derived from effective strain. It can be used for both materially and geometrical nonlinear problems. In this chapter, the sensitivity of strain energy for end-loaded, large deflection

beam is studied to verify the accuracy of the proposed method.

4.2 Formulation of deflections

In this section, the equations of deflections will be derived for a end-loaded beam with both non-follower and with follower loading . The derivation is based on the fundamental Bernoulli-Euler theorem which states that the curvature is proportional to the bending moment. It is assumed that bending does not alter the length of the beam. A cantilever beam with both non-follower and follower end loads are discussed in this section.

4.2.1 Cantilever beam with transverse(non-follower) end force

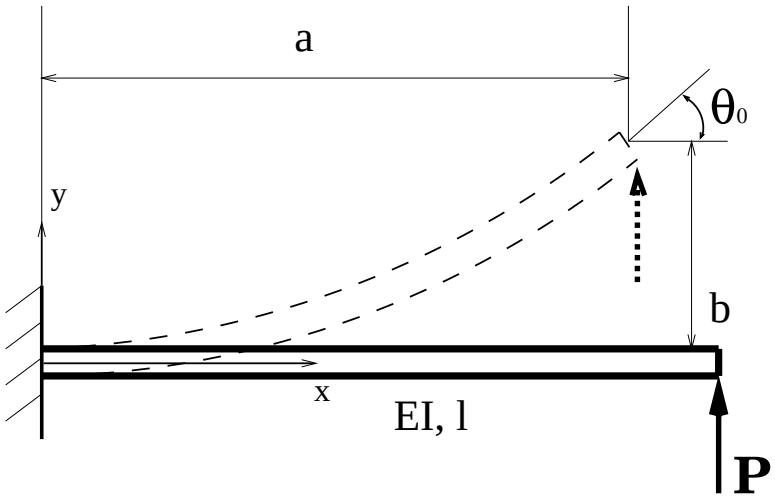

Figure 4.1: Cantilever beam with end force(non-follower)

When considering a long, thin cantilever beam, let L denote the length of beam, a the horizontal component of the displacement of the loaded end of the beam, b the corresponding vertical displacement, P the concentrated vertical load at the free end, using the exact equation for curvature, the beam equation can be written as

$$M = EI\frac{d\theta}{ds} = EI\frac{\frac{d^2y}{d^2x}}{\left(1+\left(\frac{dy}{dx}\right)^2\right)^{3/2}} \tag{4.1}$$

where M is the moment, $d\theta/ds$ the rate of change of angular deflection along the length of the beam, y the transverse deflection, x the coordinate along the undeformed beam axis, and EI the flexural rigidity . For large deflection, the internal moment at any

point in the beam is given by

$$M = P(a - x) \tag{4.2}$$

The governing equation of the beam may be written as

$$\frac{d\theta}{ds} = \frac{P}{EI}(a - x) \tag{4.3}$$

and

$$\frac{d^2\theta}{ds^2} = -\frac{P}{EI}\frac{dx}{ds} \tag{4.4}$$

or

$$\frac{d^2\theta}{ds^2} = -\frac{P}{EI}\cos\theta \tag{4.5}$$

Integrating yields

$$\frac{1}{2}\left(\frac{d\theta}{ds}\right)^2 = -\frac{P}{EI}\sin\theta + C_1 \tag{4.6}$$

The constant C_1 can be evaluated by observing that the curvature at the loaded end is zero. Then if θ_0 is the corresponding angle of slope

$$\frac{d\theta}{ds} = \sqrt{2}\frac{\alpha}{L}\sqrt{\sin\theta_0 - \sin\theta} \tag{4.7}$$

where

$$\alpha^2 = \frac{PL^2}{EI} \tag{4.8}$$

The value of θ_0 can not be found directly from this equation but it is implied by the requirement that the beam be inextensible, so that

$$\sqrt{2}\alpha = \int_0^{\theta_0} \frac{d\theta}{\sqrt{\sin\theta_0 - \sin\theta}} \tag{4.9}$$

The angular deflection for any point, final vertical and horizontal positions may be found by using the relation $ds = dx/\cos\theta = dy/\sin\theta$ as

$$\frac{s}{L} = \frac{\sqrt{2\sin\theta}}{\alpha} \tag{4.10}$$

$$\frac{a}{L} = \frac{\sqrt{2\sin\theta_0}}{\alpha} \tag{4.11}$$

$$\frac{b}{L} = \frac{1}{\sqrt{2}\alpha}\int_0^{\theta_0} \frac{\sin\theta d\theta}{\sqrt{\sin\theta_0 - \sin\theta}} \tag{4.12}$$

By similar derivations, we can obtain the expressions of nodal angular deflections for the beam with discrete material properties(Fig. 2) as

$$\sqrt{2}\alpha_1 = \int_{\theta_1}^{\theta_0} \frac{d\theta}{\sqrt{\sin\theta_0 - \sin\theta}}$$

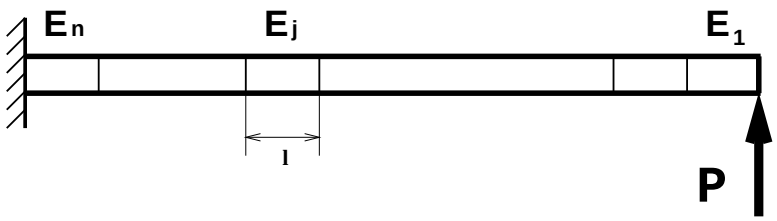

Figure 4.2: Cantilever beam with end force(non-follower)

$$\begin{aligned}\sqrt{2}\alpha_i &= \int_{\theta_i}^{\theta_{i-1}} \frac{d\theta}{\sqrt{\sum_{j=1}^{i-1}\frac{E_i}{E_j}(\sin\theta_{j-1}-\sin\theta_j)+\sin\theta_j-\sin\theta}} \\ \sqrt{2}\alpha_n &= \int_{0}^{\theta_{n-1}} \frac{d\theta}{\sqrt{\sum_{j=1}^{n-1}\frac{E_n}{E_j}(\sin\theta_{j-1}-\sin\theta_j)+\sin\theta_j-\sin\theta}} \end{aligned} \tag{4.13}$$

where l denotes the length of each element, E_i and θ_i Young's Modulus and nodal angular deflection, $\alpha_i^2 = \frac{Pl^2}{E_i I}$.

The angular deflection for any point can be obtained as

$$\begin{aligned}\frac{\sqrt{2}\alpha_1(s-s_1)}{l} &= \int_{\theta}^{\theta_0} \frac{d\theta}{\sqrt{\sin\theta_0-\sin\theta}} \quad \text{when} \quad s_1 \le s \\ \frac{\sqrt{2}\alpha_i(s-s_i)}{l} &= \int_{\theta_i}^{\theta} \frac{d\theta}{\sqrt{\sum_{j=1}^{i-1}\frac{E_i}{E_j}(\sin\theta_{j-1}-\sin\theta_j)+\sin\theta_j-\sin\theta}} \\ &\quad \text{when} \quad s_i \le s \le s_{i-1} \quad i=2,3,...,n-1 \\ \sqrt{2}\alpha_n &= \int_{\theta}^{\theta_{n-1}} \frac{d\theta}{\sqrt{\sum_{j=1}^{n-1}\frac{E_n}{E_j}(\sin\theta_{j-1}-\sin\theta_j)+\sin\theta_j-\sin\theta}} \\ &\quad \text{when} \quad s \le s_{n-1} \end{aligned} \tag{4.14}$$

The final vertical and horizontal positions may be found by using the relation $ds = dx/\cos\theta = dy/\sin\theta$ as

$$\frac{a}{l} = \frac{\sqrt{2(\sin\theta_0-\sin\theta_1)}}{\alpha_1} \tag{4.15}$$

$$\frac{b}{l} = \frac{1}{\sqrt{2}\alpha_1}\int_{\theta_1}^{\theta_0} \frac{\sin\theta d\theta}{\sqrt{\sin\theta_0-\sin\theta}} \tag{4.16}$$

4.2.2 Cantilever beam with transverse(with-follower) end force

For follower loading(Fig. 3), the internal moment at any point in the beam is given by

$$M = P[\cos\theta_0(a-x)+\sin\theta_0(b-y)] \tag{4.17}$$

The governing equation of the beam may be written as

$$\frac{d\theta}{ds} = \frac{P}{EI}[\cos\theta_0(a-x)+\sin\theta_0(b-y)] \tag{4.18}$$

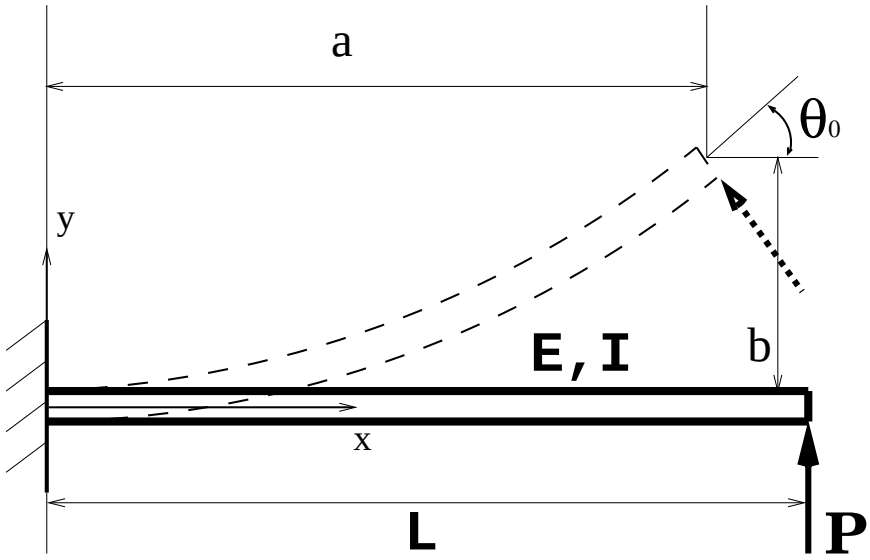

Figure 4.3: Cantilever beam with end force(with follower)

and

$$\frac{d^2\theta}{ds^2} = -\frac{P}{EI}[\frac{dx}{ds}\cos\theta_0 + \frac{dy}{ds}\sin\theta_0] \tag{4.19}$$

or

$$\frac{d^2\theta}{ds^2} = -\frac{P}{EI}[\cos\theta\cos\theta_0 + \sin\theta\sin\theta_0] \tag{4.20}$$

Integrating yields

$$\frac{1}{2}(\frac{d\theta}{ds})^2 = \frac{P}{EI}\sin(\theta_0 - \theta) + C_1 \tag{4.21}$$

Boundary conditions for this problem are

$$\begin{aligned} s &= 0, \theta = 0 \\ s &= L, \theta = \theta_0 \\ \theta &= \theta_0, d\theta/ds = 0 \end{aligned} \tag{4.22}$$

By substituting Eq (4.22) in Eq (4.21), we obtain,

$$\sqrt{2}\alpha = \int_0^{\theta_0} \frac{d\theta}{\sqrt{\sin(\theta_0 - \theta)}} \tag{4.23}$$

With the angular deflection of any point, the nonlinear solutions for a and b are

$$\frac{s}{L} = \frac{1}{\sqrt{2}\alpha}\int_\theta^{\theta_0} \frac{\sin\theta d\theta}{\sqrt{\sin(\theta_0 - \theta)}} \tag{4.24}$$

$$\frac{a}{L} = \frac{1}{\sqrt{2}\alpha}\int_0^{\theta_0} \frac{\sin\theta d\theta}{\sqrt{\sin(\theta_0 - \theta)}} \tag{4.25}$$

$$\frac{b}{L} = \frac{1}{\sqrt{2}\alpha}\int_0^{\theta_0} \frac{\cos\theta d\theta}{\sqrt{\sin(\theta_0 - \theta)}} \tag{4.26}$$

where

$$\alpha^2 = \frac{PL^2}{EI} \tag{4.27}$$

For the case with discrete material properties, we can obtain the nodal angular deflection similarly

$$\begin{aligned}
\sqrt{2}\alpha_1 &= \int_{\theta_1}^{\theta_0} \frac{d\theta}{\sqrt{\sin(\theta_0-\theta)}} \\
\sqrt{2}\alpha_i &= \int_{\theta_i}^{\theta_{i-1}} \frac{d\theta}{\sqrt{\sum_{j=1}^{i-1}(\frac{E_i}{E_j}-\frac{E_i}{E_{j+1}})\sin(\theta_0-\theta_j)+\sin(\theta_0-\theta)}} \\
\sqrt{2}\alpha_n &= \int_{0}^{\theta_{n-1}} \frac{d\theta}{\sqrt{\sum_{j=1}^{n-1}(\frac{E_n}{E_j}-\frac{E_n}{E_{j+1}})\sin(\theta_0-\theta_j)+\sin(\theta_0-\theta)}}
\end{aligned} \tag{4.28}$$

where $\alpha_i^2 = \frac{Pl^2}{E_i I}$, l the length of each element, E_i and θ_i Young's Modulus and nodal angular deflection. The angular deflection for any point is obtained as

$$\begin{aligned}
\frac{\sqrt{2}\alpha_1(s-s_1)}{l}al &= \int_{\theta}^{\theta_0} \frac{d\theta}{\sqrt{\sin(\theta_0-\theta)}} \quad \text{when} \quad s_1 \le s \\
\frac{\sqrt{2}\alpha_i(s-s_i)}{l} &= \int_{\theta}^{\theta_{i-1}} \frac{d\theta}{\sqrt{\sum_{j=1}^{i-1}(\frac{E_i}{E_j}-\frac{E_i}{E_{j+1}})\sin(\theta_0-\theta_j)+\sin(\theta_0-\theta)}} \\
&\quad \text{when} \quad s_i \le s \le s_{i-1} \quad i = 2,3,...,n-1 \\
\frac{\sqrt{2}\alpha_n s}{l} &= \int_{0}^{\theta_{n-1}} \frac{d\theta}{\sqrt{\sum_{j=1}^{n-1}(\frac{E_n}{E_j}-\frac{E_n}{E_{j+1}})\sin(\theta_0-\theta_j)+\sin(\theta_0-\theta)}} \\
&\quad \text{when} \quad s \le s_{n-1}
\end{aligned} \tag{4.29}$$

The final vertical and horizontal positions may be found as

$$\frac{a}{l} = \frac{1}{\sqrt{2}\alpha_1}\int_{\theta_1}^{\theta_0} \frac{\cos\theta d\theta}{\sqrt{\sin(\theta_0-\theta)}} \tag{4.30}$$

$$\frac{b}{l} = \frac{1}{\sqrt{2}\alpha_1}\int_{\theta_1}^{\theta_0} \frac{\sin\theta d\theta}{\sqrt{\sin(\theta_0-\theta)}} \tag{4.31}$$

Based on the above the results, we will discuss the sensitivity analysis of strain energy in next section.

4.3 Sensitivity of total strain energy

To verify the accuracy of sensitivity calculation by the effective strain based method, in this section, the expressions of sensitivity of total strain energy are derived by both classical approach and proposed method.

4.3.1 Classical approach of sensitivity of total strain energy

The sensitivity of total strain energy can be derived by directly differentiating the equation of total strain energy. This results can give us an exact solution even though the derivations are very lengthy.

Non-follower loading

The total strain energy for the beam may be written as

$$\begin{aligned} U &= \int_0^l \frac{M^2}{2EI} ds \\ &= \frac{P^2}{2EI} \int_0^L (a - s\cos\theta)^2 ds \end{aligned} \tag{4.32}$$

Sensitivity of strain energy can be derived from the above equation as

$$\frac{dU}{dh} = \frac{P^2}{2EI} \int_0^L \{[2(a - s\cos\theta)(\frac{da}{dh} + s\sin\theta\frac{d\theta}{dh}) - \frac{(a - s\cos\theta)^2}{E}\frac{dE}{dh}\} ds \tag{4.33}$$

where h is the design variable, a and $da/d\theta$ are determined by Eq (4.11), and θ and $d\theta/dh$ are determined by Eq (4.11) or Eq (4.12).

For discrete material properties, total strain energy is written as

$$\begin{aligned} U &= \sum_{i=1}^{n} \int_{s_{i-1}}^{s_i} \frac{M^2}{2E_i I} ds \\ &= \sum_{i=1}^{n} \int_{s_{i-1}}^{s_i} \frac{P^2(a - x)^2}{2E_i I} ds \\ &= \sum_{i=1}^{n} \int_{s_{i-1}}^{s_i} \frac{P^2(a - s\cos\theta)^2}{2E_i I} ds \end{aligned} \tag{4.34}$$

Sensitivity of strain energy can be derived from the above equation as

$$\begin{aligned} \frac{dU}{dh_j} &= \sum_{i=1, i\neq j}^{n} \int_{s_{i-1}}^{s_i} \frac{P^2(a - s\cos\theta)}{E_i I} (\frac{da}{dh_j} + s\sin\theta\frac{d\theta}{dh_j}) ds \\ &\quad + \int_{s_{j-1}}^{s_j} \{\frac{P^2(a - s\cos\theta)}{E_j I} (\frac{da}{dh_j} + s\sin\theta\frac{d\theta}{dh_j}) \\ &\quad - \frac{P^2(a - s\cos\theta)^2}{2E_j I}\frac{dE_j}{dh_j}\} ds \end{aligned} \tag{4.35}$$

In the Eq (4.35), a and da/dh are determined by Eq (4.15), and θ and $d\theta/dh$ are determined by Eq (4.15) or Eq (4.16).

Follower loading

The total strain energy for the beam may be written as

$$\begin{aligned} U &= \int_0^l \frac{M^2}{2EI} ds \\ &= \frac{P^2}{2EI} \int_0^L \left[(a - s\cos\theta)\cos\theta_0 + (b - s\sin\theta)\sin\theta_0\right]^2 ds \end{aligned} \tag{4.36}$$

Sensitivity of strain energy can be derived from the above equation as

$$\begin{aligned} \frac{dU}{dh} &= \frac{P^2}{2EI} \int_0^L \{2[(a - s\cos\theta)\cos\theta_0 + (b - s\sin\theta)\sin\theta_0][(\frac{da}{dh} \\ &\quad + \sin\theta_0 \frac{d\theta_0}{dh})\cos\theta_0 - (a - s\cos\theta)\sin\theta_0 \frac{d\theta_0}{dh} + (\frac{db}{dh} - s\cos\theta\frac{d\theta}{dh})\sin\theta_0 \\ &\quad + (b - s\sin\theta)\cos\theta_0 \frac{d\theta_0}{dh}] \\ &\quad - \frac{\left[(a - s\cos\theta)\cos\theta_0 + (b - s\sin\theta)\sin\theta_0\right]^2}{E} \frac{dE}{dh}\} ds \end{aligned} \tag{4.37}$$

where h is the design variable, a and $da/d\theta$ are determined by Eq (4.24), b and $db/d\theta$ are determined by Eq (4.25), and θ and $d\theta/dh$ are determined by Eq (4.24) or Eq (4.25).

For discrete material properties, total strain energy is written as

$$\begin{aligned} U &= \sum_{i=1}^{n} \int_{s_{i-1}}^{s_i} \frac{M^2}{2E_i I} ds \\ &= \sum_{i=1}^{n} \int_{s_{i-1}}^{s_i} \frac{P^2[\cos\theta_0(a - x) + \sin\theta_0(b - y)]^2}{2E_i I} ds \\ &= \sum_{i=1}^{n} \int_{s_{i-1}}^{s_i} \frac{P^2[\cos\theta_0(a - s\cos\theta) + \sin\theta_0(b - s\sin\theta)]^2}{2E_i I} ds \end{aligned} \tag{4.38}$$

Sensitivity of strain energy can be derived from the above equation as

$$\begin{aligned} \frac{dU}{dh_j} &= \sum_{i=1, i\neq j}^{n} \int_{s_{i-1}}^{s_i} \{2[(a - s\cos\theta)\cos\theta_0 + (b - s\sin\theta)\sin\theta_0][(\frac{da}{dh_i} \\ &\quad + \sin\theta_0 \frac{d\theta_0}{dh_i})\cos\theta_0 - (a - s\cos\theta)\sin\theta_0 \frac{d\theta_0}{dh_i}\} ds + \int_{s_{j-1}}^{s_j} \{2[(a - s\cos\theta)\cos\theta_0 \\ &\quad + (b - s\sin\theta)\sin\theta_0][(\frac{da}{dh_j} + \sin\theta_0 \frac{d\theta_0}{dh_j})\cos\theta_0 - (a - s\cos\theta)\sin\theta_0 \frac{d\theta_0}{dh_j} \\ &\quad + (\frac{db}{dh_j} - s\cos\theta\frac{d\theta}{dh_j})\sin\theta_0 + (b - s\sin\theta)\cos\theta_0 \frac{d\theta_0}{dh_j}] \\ &\quad - \frac{\left[(a - s\cos\theta)\cos\theta_0 + (b - s\sin\theta)\sin\theta_0\right]^2}{E_j} \frac{dE_j}{dh_j}\} ds \end{aligned} \tag{4.39}$$

In the Eq (4.39), a and da/dh are determined by Eq (4.15), b and db/dh are determined by Eq (4.16), and θ and $d\theta/dh$ determined by Eq (4.15) or Eq (4.16).

4.3.2 Effective-strain based method for sensitivity of total strain energy

General sensitivity of strain energy was derived in terms of effective strains by the point of energy-consistent view as

$$\frac{dU}{dh} = \{\int_V [\int_{\overline{\varepsilon}} f(\overline{\varepsilon}(h))d\overline{\varepsilon} - \frac{f^2(\overline{\varepsilon}(h))}{f'(\overline{\varepsilon}(h))}]dV\}\frac{\partial E(h)}{\partial h} \tag{4.40}$$

where h is the design variable and f depends on the relation of effective stress and effective strain. For large deflection beam with linear elastic materials, we have

$$f = \overline{\varepsilon} = \varepsilon_x \tag{4.41}$$

The Eq (4.40) thus can be reduced to

$$\begin{aligned} \frac{dU}{dh} &= -\int_V \frac{1}{2}{\varepsilon_x}^2 dV \frac{dE}{dh} \\ &= -\int_0^L \frac{M^2}{2E^2 I} ds \frac{dE}{dh} \end{aligned} \tag{4.42}$$

The localized sensitivity formulation is written as

$$\frac{dU}{dh_j} = -\int_{s_{j-1}}^{s_j} \frac{M^2}{2E_j^2 I} ds \frac{dE_j}{dh_j} \tag{4.43}$$

Non-Follower loading

Sensitivity of strain energy can be derived from the above equation as

$$\frac{dU}{dh} = \frac{P^2}{2E^2 I}\int_0^L (a - s\cos\theta)^2 ds \frac{dE}{dh} \tag{4.44}$$

Localized sensitivity of strain energy can be derived from the above equation as

$$\frac{dU}{dh_j} = -\frac{P^2}{2E_j^2 I}\int_{s_{j-1}}^{s_j} (a - s\cos\theta)^2 ds \frac{dE_j}{dh_j} \tag{4.45}$$

Follower loading

Sensitivity of strain energy can be derived from the above equation as

$$\frac{dU}{dh} = \frac{P^2}{2E^2 I}\int_0^L [\cos\theta_0(a - s\cos\theta) + \sin\theta_0(b - s\sin\theta)]^2 ds \frac{dE}{dh} \tag{4.46}$$

Localized sensitivity of strain energy can be derived from the above equation as

$$\frac{dU}{dh_j} = -\frac{P^2}{2E_j^2 I}\int_{s_{j-1}}^{s_j} [\cos\theta_0(a - s\cos\theta) + \sin\theta_0(b - s\sin\theta)]^2 ds \frac{dE_j}{dh_j} \tag{4.47}$$

4.4 Examples

In this section, to evaluate the accuracy of the new method, numerical results obtained by the proposed method are compared with those from classical method and a finite difference derivative. XMAPLE and MSC/NASTRAN commercial finite element codes for geometric nonlinearity are used to obtain standard structural analysis results.

In this example, we assume the material modulus is a function of design variables. $E_i = E_{i0}g(h)$ with E_{i0} as the modulus constant of i-th element. We choose $g(h) = h^2$ for this example but any continuous function can be used.

The results in Table 1 represent the sensitivities of total strain energy of four different elements calculated by the classical solution, effective based method and finite difference derivative method for non-follower loading. Maximum vertical and horizontal deflection at the end of beam are 0.55 and 0.2 times the total length of the beam.

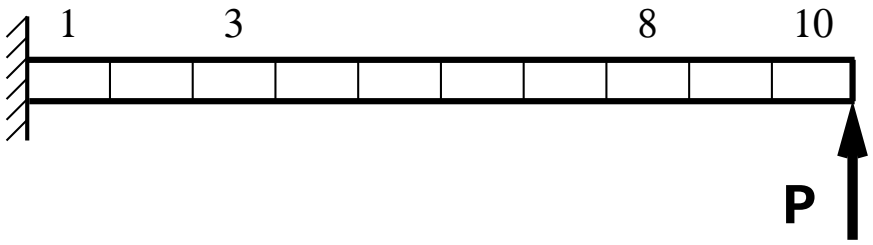

Figure 4.4: Cantilever beam with end force

No. of elem	Analytical(A)	New method(N)	Finite difference(F)	A&N	A&F
1	-7.492111e+01	-7.453414e+01	-7.604912e+01	0.5%	1.4%
3	-3.972313e+01	-3.952429e+01	-3.89443e+01	0.5%	1.9%
8	-2.159211e+01	-2.145332e+01	-2.183221e+01	0.6%	1.1%
10	-4.021334e-00	-4.002211e-00	-4.093211e-00	0.5%	1.7%

Table 4.1: **Comparison of the results(non-follower)**

No. of elem	Analytical(A)	New method(N)	Finite difference(F)	A&N	A&F
1	-8.383412e+01	-8.341231e+01	-8.294231e+01	0.5%	1.1%
3	-4.230053e+01	-4.215674e+01	-4.174123e+01	0.4%	1.3%
8	-3.145299e+01	-3.122224e+01	-3.193111e+01	0.7%	1.5%
10	-6.942222e+00	-6.902113e-00	-6.792112e-00	0.6%	2.2%

Table 4.2: **Comparison of the results (with-follower)**

The results in Table 2 represent the sensitivities of total strain energy of four different elements calculated by the classical solution, effective based method and finite difference derivative method with follower loading. Maximum vertical and horizontal deflection at the end of beam are 0.63 and 0.27 times the total length of the beam.

From the results in Table 1 and 2, it is clear that sensitivity calculations from the effective strain based method are in even closer agreement than finite difference results with classical results.

4.5 Conclusion

The effective-strain sensitivity analysis method is based on the energy consistent view. It is not only computationally efficient, but also of very good accuracy marker for large deflection problems. The numerical results demonstrated a high incidence of agreement between the results for effective-strain method, classical method and finite difference approach.

Chapter 5

Sensitivity Analysis for Reliability-based Structural Design

5.1 Introduction

In a structural optimization problem with the external loads and the structural strengths being treated as random variables, optimization becomes more complicated than ordinary deterministic designs because of the difficulty in the sensitivity analysis of the structural reliability or structural failure probability.

The first attempt to analyze the importance of sensitivity analysis in structural reliability was made by Modes in 1970. In this chapter, special emphasis is placed on cost sensitivity studies to illustrate the influence on the reliability-based design of the idealizations of the probabilistic model, the analysis errors, and the choice of statistical parameters. In 1985, Frangopol explored in depth the sensitivity of both the overall reliability and the optimum solutions of redundant ductile structures with relation structure of the random loads and strengths, and the method used for global reliability evaluation. Recently, the hybrid design sensitivity analysis method (Chang et al. 1997) was employed for the mixed approach for probabilistic structural durability.

In reliability analysis, the Monte Carlo simulation method is often employed when the analytical solution is not attainable and the failure domain cannot be expressed or approximated by an analytical form. This is mainly the case in problems of complex nature with a large number of basic variables, to which all other reliability analysis methods are not applicable. Although the mathematical formulation of the Monte Carlo simulation method is relatively simple and the method has the capability of handling practically any possible case regardless of its complexity, the computational effort involved in conventional Monte Carlo simulation is excessive. The goal of this chapter is to derive a closed-form solution of design sensitivity for structural reliability. That is, we want to deal with sensitivity for reliability-based design problems by the

effective models defined from an energy consistent point of view.

5.2 Evaluation of structural reliability

Assume that the random maximum stress, S_m and the random endurance strength, $\overline{S}_e$ are known and described by known probability distributions. If these distributions are specified in terms of the probability density functions, $f_{S_m}(r)$ and $f_{S_e}(r)$, respectively, then the measure of risk is the probability of the "failure" event($S_m \leq S_e$). Thus Freundenthal stated in 1966:

$$\begin{aligned} p_f = P(\text{failure}) &= P(S_m \leq S_e) \\ &= \int_0^\infty [\int_0^S f_R(r)dr] f_s(s)ds \\ &= \int_0^\infty F_R(s) f_S(s)ds \end{aligned} \tag{5.1}$$

in which $F_R()$ = the cumulative distribution function of R. When the maximum stress is $S_m = s$, the probability of failure is clearly $F_R(s)$. Eq (5.1) simply includes all possible values of S, with their respective probabilities.

If S_m and S_e follow normal distribution, reliability may be expressed as

$$R = \frac{1}{\sqrt{2\pi}} \int_{z_1}^\infty e^{-z^2/2} dz \tag{5.2}$$

where the lower limit of integration, z_1, is found from the principles of strength based reliability as

$$z_1 = -\frac{\mu_{S_e} - \mu_{S_m}}{\sqrt{\sigma_{S_e}^2 + \sigma_{S_m}^2}} \tag{5.3}$$

where μ_{S_m} and $\sigma_{S_m}^2$ are mean and deviation of maximum stress, μ_{S_e} and $\sigma_{S_e}^2$ are mean and deviation of endurance strength.

5.3 Modeling of nonlinear elasticity

In this section, the nonlinear elasticity modeled by effective strain and effective stress for generalized material nonlinearity are briefly introduced. The effective strain is defined as

$$\overline{\varepsilon}^2 = \boldsymbol{\varepsilon}^T \boldsymbol{C_0} \boldsymbol{\varepsilon} \tag{5.4}$$

where $\boldsymbol{C_0}$ is a symmetric, positive definite and dimension-less matrix. Generally, the nonlinear stress may be an arbitrary function of the strain.

$$\overline{\sigma} = Ef(\overline{\varepsilon}) \tag{5.5}$$

where E is the modulus for a reference state and a function of design variable h. $f(\overline{\varepsilon})$ should be a increasing function with respect to $\overline{\varepsilon}$. The strain energy density, the stress energy density and the virtual work are expressed in terms of effective strains as

$$\begin{aligned} u &= E\int f(\overline{\varepsilon})d\overline{\varepsilon} \\ u^c &= \int E\overline{\varepsilon}f'(\overline{\varepsilon})d\overline{\varepsilon} \\ w &= E\overline{\varepsilon}f(\overline{\varepsilon}) \end{aligned} \tag{5.6}$$

where $f'(\overline{\varepsilon}) = df(\overline{\varepsilon})/d\overline{\varepsilon}$.

The derivative of effective strains can be derived as

$$\frac{\partial\overline{\varepsilon}(h)}{\partial h} = -\frac{f(\overline{\varepsilon})}{E(h)}\frac{E'(h)}{f'(\varepsilon)} \tag{5.7}$$

5.4 Sensitivity analysis of structural reliability

The reliability is determined by the means and deviations of the maximum stress and the endurance strength. Generally, the deterministic form of endurance strength can be presented by stochastic variables(Mischke, 1987). Therefore, the derivative for endurance strength can be obtain by the deterministic form. In the first part of this section, we will discuss an approximate solution for means and standard deviations for general nonlinear function of random variables. Then we will study the sensitivity solution for the von Mises stress(normally used for measuring the maximum stress) based on the effective strain introduced in section 3.

5.4.1 Means and standard deviations of general nonlinear function of random variables

The approximations of the mean and standard deviations of a general nonlinear function of several random variables can obtained by means of the "partial derivative rule"(Rao, 1992). Consider a nonlinear function of several random variables as

$$Y = g(X_1, X_2, ..., X_n) \tag{5.8}$$

Expanding the function in a Taylor's series about the mean values and neglecting terms involving second and higher order derivations yields

$$Y = g(\mu_1, \mu_2, ..., \mu_n) + \sum_{i=1}^{n} \frac{\partial g}{\partial X_i}|_{\mu_1,\mu_2,...,\mu_n}(X_i - \mu_i) \tag{5.9}$$

Since $g(\mu_1, \mu_2, ...\mu_n)$ and $\partial g/\partial X_i|_{\mu_1,\mu_2,...,\mu_n}$ are constants, the mean value of Y may be approximated as

$$\begin{aligned} \mu_Y &= E[g(\mu_1, \mu_2, ..., \mu_n) + \sum_{i=1}^{n} \frac{\partial g}{\partial X_i}|_{\mu_1,\mu_2,...,\mu_n}(X_i - \mu_i)] \\ &= g(\mu_1, \mu_2, ..., \mu_n) + \sum_{i=1}^{n} \frac{\partial g}{\partial X_i}|_{\mu_1,\mu_2,...,\mu_n} E(X_i - \mu_i) \\ &= g(\mu_1, \mu_2, ..., \mu_n) \end{aligned} \tag{5.10}$$

From Eq (5.10), we can obtain

$$\begin{aligned} Y^2 &= g^2(\mu_1, \mu_2, ..., \mu_n) + 2g(\mu_1, \mu_2, ..., \mu_n) \sum_{i=1}^{n} \frac{\partial g}{\partial X_i}|_{\mu_1,\mu_2,...,\mu_n} E(X_i - \mu_i) + \\ &\quad [\sum_{i=1}^{n} \frac{\partial g}{\partial X_i}|_{\mu_1,\mu_2,...,\mu_n} E(X_i - \mu_i)]^2 \\ &= g^2(\mu_1, \mu_2, ..., \mu_n) + 2g(\mu_1, \mu_2, ..., \mu_n) \sum_{i=1}^{n} \frac{\partial g}{\partial X_i}|_{\mu_1,\mu_2,...,\mu_n} E(X_i - \mu_i) + \\ &\quad \sum_{i=1}^{n} (\frac{\partial g}{\partial X_i}|_{\mu_1,\mu_2,...,\mu_n})^2 E(X_i^2 - 2X_i\mu_i + \mu_i^2) + \\ &\quad \sum_{i=1}^{n} \sum_{j=1, j\neq i}^{n} \frac{\partial g}{\partial X_i}|_{\mu_1,\mu_2,...,\mu_n} \frac{\partial g}{\partial X_j}|_{\mu_1,\mu_2,...,\mu_n} E(X_i - \mu_i)E(X_j - \mu_j) \end{aligned} \tag{5.11}$$

By reorganizing Eq (5.11), the variance Y may be approximated as

$$\begin{aligned} \sigma_Y^2 &= E(Y_2) - E(Y)^2 \\ &= \sum_{i=1}^{n} (\frac{\partial g}{\partial X_i})^2 |_{\mu_1,\mu_2,...,\mu_n} \sigma_{X_i}^2 + \sum_{i=1}^{n} \sum_{j=1, i=j}^{n} \frac{\partial g}{\partial X_i}|_{\mu_1,\mu_2,...,\mu_n} \frac{\partial g}{\partial X_j} \sigma_{X_i X_j}^2 \end{aligned} \tag{5.12}$$

Since the variables involved are statistically independent

$$\sigma_Y^2 = \sum_{i=1}^{n} (\frac{\partial g}{\partial X_i})^2 |_{\mu_1,\mu_2,...,\mu_n} \sigma_{X_i}^2 \tag{5.13}$$

the mean and standard deviation for the endurance strength can be easily obtained from the above results, and the deterministic form of endurance strength is given.

5.4.2 Sensitivity analysis based on the effective model

The maximum stress can be measured by the von Mises stress, defined by

$$S_m^2 = \frac{3}{2} \boldsymbol{S_d}^T \boldsymbol{S_d} \tag{5.14}$$

where $\boldsymbol{S_d}$ is the vector of deviatoric stresses, i.e. the hydrostatic pressure is eliminated. Pedersen(1987) showed that this deviatoric stress vector can be obtained by a projection with the projection matrix $\boldsymbol{P}$

$$S_m^2 = \frac{3}{2}\boldsymbol{S}^T\boldsymbol{P}\boldsymbol{S} \tag{5.15}$$

where $\boldsymbol{S}$ is the vector of stresses,

$$\boldsymbol{P} = \begin{bmatrix} 2 & -1 & -1 & 0 & 0 & 0 \\ -1 & 2 & -1 & 0 & 0 & 0 \\ -1 & -1 & 2 & 0 & 0 & 0 \\ 0 & 0 & 0 & 3 & 0 & 0 \\ 0 & 0 & 0 & 0 & 3 & 0 \\ 0 & 0 & 0 & 0 & 0 & 3 \end{bmatrix} \tag{5.16}$$

Recalling the definition of effective stress,

$$\overline{S}^2 = \boldsymbol{S}^T{\boldsymbol{C_0}}^{-1}\boldsymbol{S} \tag{5.17}$$

where

$$\boldsymbol{C_0} = \frac{1-\nu}{(1+\nu)(1-2\nu)} \begin{bmatrix} 1 & \frac{\nu}{1-\nu} & \frac{\nu}{1-\nu} & 0 & 0 & 0 \\ \frac{\nu}{1-\nu} & 1 & \frac{\nu}{1-\nu} & 0 & 0 & 0 \\ \frac{\nu}{1-\nu} & \frac{\nu}{1-\nu} & 1 & 0 & 0 & 0 \\ 0 & 0 & 0 & \frac{1-2\nu}{2(1-\nu)} & 0 & 0 \\ 0 & 0 & 0 & 0 & \frac{1-2\nu}{2(1-\nu)} & 0 \\ 0 & 0 & 0 & 0 & 0 & \frac{1-2\nu}{2(1-\nu)} \end{bmatrix} \tag{5.18}$$

ν is the Poisson's ratio. Comparing Eq (5.17) to Eq (5.15), $S_m^2 = \overline{S}^2$ for the compliance matrix that corresponds to an isotropic and incompressible material.

Generally, $\overline{S}$ can be expressed as a function of random variables(Modulus and size parameters),

$$\overline{S} = Ef(\bar{\varepsilon}(E(h), t, ...)) \tag{5.19}$$

where E is the Modulus, $\bar{\varepsilon}$ the effective strain and t is size parameter such as thickness. Based on section 3, we already know

$$\frac{\partial\bar{\varepsilon}}{\partial H} = -\frac{f(\bar{\varepsilon})}{Hf'(\bar{\varepsilon})} \tag{5.20}$$

where H can be Modulus or size parameter. If H is Modulus, then the derivative of effective stress to Modulus can be written as

$$\frac{d\overline{S}}{dh} = [\int f(\overline{\varepsilon})d\overline{\varepsilon} + Ef(\overline{\varepsilon})\frac{\partial\overline{\varepsilon}}{\partial E}]\frac{dE}{dh} \tag{5.21}$$

By inserting Eq (5.20) in Eq (5.21), we can get

$$\frac{d\overline{S}}{dh} = [\int f(\overline{\varepsilon})d\overline{\varepsilon} - f^2(\overline{\varepsilon})]\frac{dE}{dh} \tag{5.22}$$

We can also can write the following if H is size parameter such as thickness:

$$\frac{\partial\overline{S}}{\partial t} = Ef(\overline{\varepsilon})\frac{\partial\overline{\varepsilon}}{\partial t} \tag{5.23}$$

By inserting Eq (5.20) in Eq (5.23), we can get

$$\frac{\partial\overline{S}}{\partial t} = -\frac{E}{t}\frac{f^2(\overline{\varepsilon})}{f'(\overline{\varepsilon})} \tag{5.24}$$

5.5 Numerical results

In this section, a 2-D and a 3-D numerical examples with both geometric and material nonlinearity are presented to demonstrate the application for the proposed method in sensitivity analysis. ANSYS commercial finite element codes for geometric nonlinearity are used to obtain standard structural analysis results .

To evaluate the accuracy of the new method, numerical results obtained by the proposed method are compared with those from a finite difference derivative. For each example, we assume the material modulus is a function of design variables.

$$E = E_{i0}g(h) \tag{5.25}$$

when E_{i0} is random modulus constant of element i we only consider the mean of E_{i0} as design variables.

$$g(h) = h^2 \qquad \text{with} \;\; 0 \leq h \leq 1 \tag{5.26}$$

The following three different material behaviors are studied in each example:

Case 1: The softening material modeled by the power-law stress-strain relation,

$$f(\overline{\varepsilon}) = \overline{\varepsilon}^n \qquad \text{with} \;\; n < 1. \tag{5.27}$$

The stress-strain behavior is shown in Figure 1.

Case 2: The stiffening material modeled by the power-law stress-strain relation,

$$f(\bar{\varepsilon}) = \bar{\varepsilon}^n \qquad \text{with} \quad n > 1. \tag{5.28}$$

The stress-strain behavior is shown in Figure 2.

Case 3: With typical rubber-like material behavior, the stress-strain relation can be described in the following form of a series expansion

$$f(\bar{\varepsilon}) = \bar{\varepsilon} - 40\bar{\varepsilon}^2 + 625\bar{\varepsilon}^3. \tag{5.29}$$

The stress-strain behavior is shown in Figure 3.

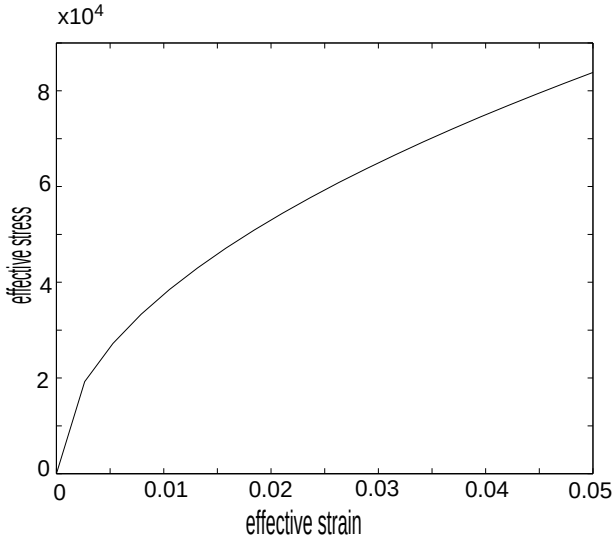

Figure 5.1: The stress-strain behavior: case 1(power law with $n < 1$)

5.5.1 Example 1: two-dimensional plane

A simple two-dimensional plane is considered as a first example to study the application and accuracy of the proposed approach. This example has 3×15 finite elements and external loads are applied to the free end of beam(Figure 3). The results in Tables 1, 2, and 3, represent the sensitivities of effective strains for four different elements calculated by the new method and finite difference derivative method, as well as their relative differences for nonlinear material behaviors of cases 1, 2, and 3, respectively. As shown in Tables 1, 2 and 3,

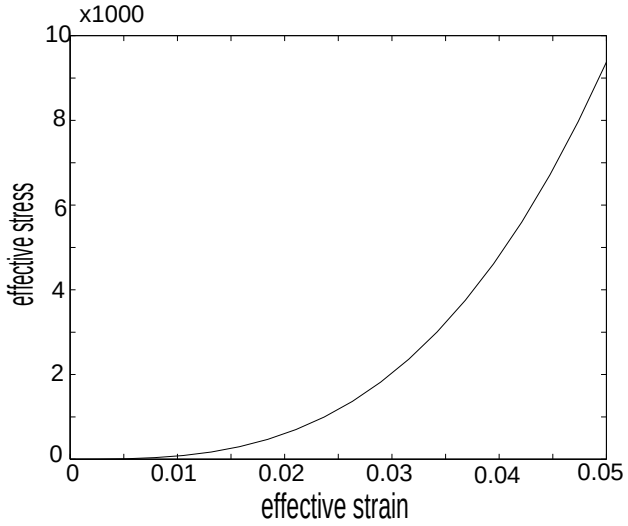

Figure 5.2: The stress-strain behavior: case 2(power law with $n > 1$)

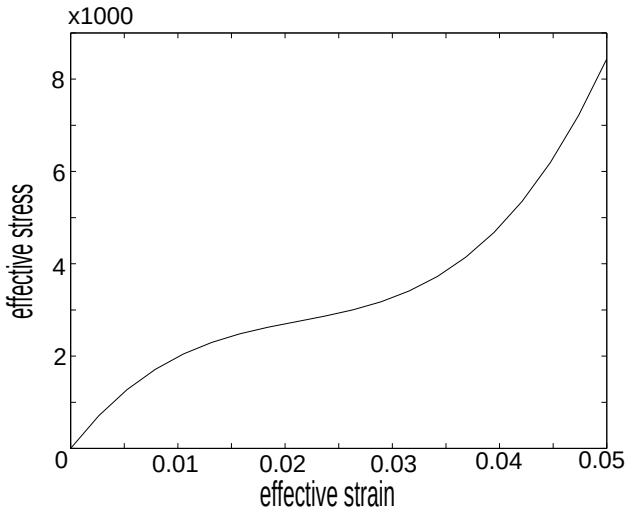

Figure 5.3: The stress-strain behavior: case 3(typical rubber behavior)

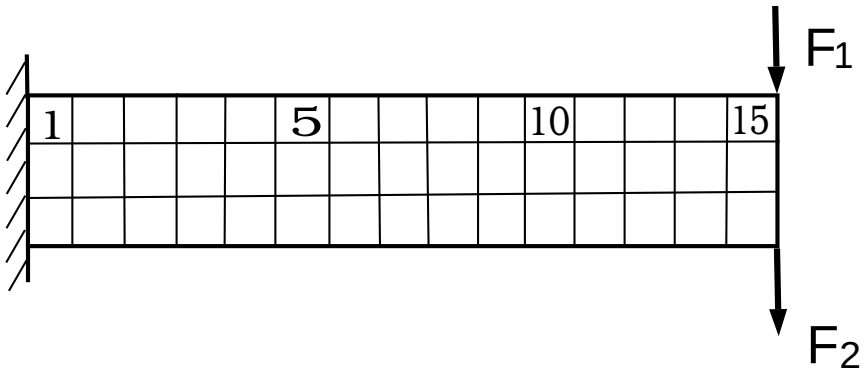

Figure 5.4: Example 1: two dimensional plane

No. of elem	New method	Finite difference derivative	The relative difference
1	-0.3244	-0.3205	1.2%
5	-0.1934	- 0.1906	1.4%
10	-0.2394	-0.2358	1.5%
15	-0.2732	-0.2694	1.4%

Table 5.1: **Comparison of the results of plane for case 1**

No. of elem	New method	Finite difference derivative	The relative difference
1	-0.03212	-0.03193	0.5%
5	-0.01833	-0.01812	1.0%
10	-0.02421	-0.02398	1.2%
15	-0.02732	-0.02694	1.2%

Table 5.2: **Comparison of the results of plane for case 2**

No. of elem	New method	Finite difference derivative	The relative difference
1	-0.0563	-0.05592	0.7%
5	-0.03942	-3.3898	1.1%
10	-0.04544	-0.04498	1.0%
15	-0.04922	-0.04867	1.1%

Table 5.3: **Comparison of the results of plane for case 3**

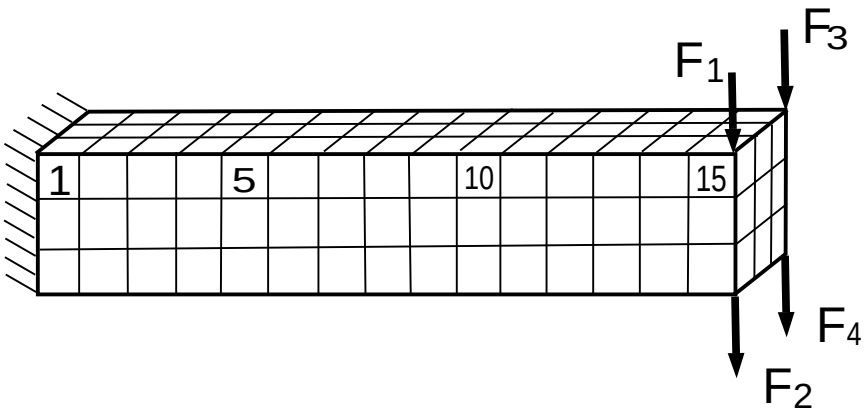

Figure 5.5: Example 2: 3-D solid

No. of elem	New method	Finite difference derivative	The relative difference
1	-0.2544	-0.2495	1.9%
5	-0.1322	-0.1284	2.8%
10	-0.1649	-0.1626	1.4%
15	-0.1817	-0.1786	1.7%

Table 5.4: **Comparison of the results of 3-D solid for case 1**

5.5.2 Example 2: 3-D solid

The second example presents a 3-D problem with $3 \times 3 \times 15$ finite elements, as external loads are applied to the free end of beam(Figure 4).

The results in Tables 4, 5, and 6 represent the sensitivities of effective strains for a 3-D solid obtained by the new method and finite different derivative method, as well as their relative differences for cases 1, 2, and 3 nonlinear material behaviors, respectively.

No. of elem	New method	Finite difference derivative	The relative difference
1	-0.03621	-0.03566	1.5%
5	-0.01034	-0.0101	2.6%
10	-0.01950	-0.01912	1.9%
15	-0.02181	-0.02141	1.8%

Table 5.5: **Comparison of the results of 3-D solid for case 2**

No. of elem	New method	Finite difference derivative	The relative difference
1	-0.04322	-0.04252	1.6%
5	-0.01934	-0.01877	2.9%
10	-0.02832	-0.02778	1.9%
15	-0.03834	-0.03761	1.9%

Table 5.6: **Comparison of the results of 3-D solid for case 3**

5.6 Conclusion

The chapter extends the effective strain based sensitivity analysis to reliability design. This method is based on the general non-linear elastic structures. It can be widely used to solve many practical problems. The advantage of this approach is its computational efficiency and high accuracy. The numerical examples demonstrated a high incidence of agreement between the results from the proposed method and those from the finite difference method.

Chapter 6

Sensitivity Analysis for Hyperelastic Material With Large Strains

6.1 Introduction

The analysis of rubber-like elastic is a challenging task in optimization of structural design due to extremely large deformations and the nearly compressible nature of rubber. In this chapter, we extend the modeling of non-linear elasticity to nonlinear hyper-elasticity. In this study, we have derived closed-form solution for sensitivity of total strain energy for nonlinear hyper-elasticity. Several numerical examples are presented to verify the results.

6.2 Generalized Approach

Sensitivity for strain energy is defined as

$$\frac{dU(\epsilon(h),h)}{dh} \tag{6.1}$$

where h is the design field and the U is total strain energy. The total strain energy is defined as:

$$U = \int_{V^0} u dV^0 \tag{6.2}$$

where u is the strain energy density referred to in the original configuration. From the analysis in chapters 2 and 3, for generalized nonlinear materials, the relation between effective stress and strain is expressed as

$$\overline{S} = E(h) f(\overline{\epsilon}(h)) \tag{6.3}$$

where E is the modulus and only dependent on design variables and f is a function of the effective strain. The strain energy density can thusly be written as

$$u = E(h) \int f(\overline{\epsilon}) d\overline{\epsilon} \tag{6.4}$$

Differentiating the total strain energy with respect to the design variable, sensitivity can be written as

$$\begin{aligned}\frac{dU}{dh} &= \int_{V^0} \frac{du}{dh} dV^0 \\ &= \int_{V^0} [(\frac{\partial u(\overline{\epsilon}(h),h)}{\partial h})_{fixed-strain} + (\frac{\partial u(\overline{\epsilon}(h),h)}{\partial \overline{\epsilon}(h)})(\frac{\partial \overline{\epsilon}(h)}{\partial h})_{fixed-h}] dV^0 \\ &= \int_{V^0} [\int f(\overline{\epsilon}) d\overline{\epsilon} \frac{\partial E}{\partial h} + E(h) f(\overline{\epsilon}(h))(\frac{\partial \overline{\epsilon}(h)}{\partial h})] dV^0 \end{aligned} \tag{6.5}$$

Using the same approach for the sensitivity analysis for nonlinear materials, the sensitivity of total strain energy can be written as

$$\begin{aligned}\frac{dU}{dh} &= \int_{V^0} [\int_{\overline{\epsilon}} f(\overline{\epsilon}(h)) d\overline{\epsilon} \frac{\partial E(h)}{\partial h} - \frac{f^2(\overline{\epsilon}(h))}{\frac{df(\overline{\epsilon}(h))}{d\overline{\epsilon}}} \frac{\partial E(h)}{\partial h}] dV^0 \\ &= \{\int_{V^0} [\int_{\overline{\epsilon}} f(\overline{\epsilon}(h)) d\overline{\epsilon} - \frac{f^2(\overline{\epsilon}(h))}{f'(\overline{\epsilon}(h))}] dV^0\} \frac{\partial E(h)}{\partial h} \end{aligned} \tag{6.6}$$

A simple and widely used elastic material for large deformation analysis is the Kirchhoff material,

$$f(\overline{\epsilon}) = \overline{\epsilon} \tag{6.7}$$

By substituting it in the Eq (6.6),

$$\frac{dU}{dh} = \int_V (\frac{\overline{\epsilon}^2}{2} - \overline{\epsilon}^2) dV \frac{\partial E}{\partial h} \tag{6.8}$$

By reorganizing it, we get

$$\frac{dU}{dh} = -\int_V \frac{\overline{\epsilon}^2}{2} dV \frac{\partial E}{\partial h} = -(\frac{\partial U}{\partial h})_{fixed-strain} \tag{6.9}$$

It can be seen from Eq (6.9) that Eq (6.6) reduces itself to the known result for linear elasticity (Pedersen, 1991)

The formulation of design sensitivity of total strain energy for finite element implementation can be obtained easily based on the above discussion.

Total strain energy for finite element forms may be represented by effective strains:

$$U = \sum_{i=1}^{N} \int_{V_i} E_i \int_{\overline{\epsilon}} f(\overline{\epsilon}) d\overline{\epsilon} dV_i \tag{6.10}$$

where E_i, V_i are modulus and the volume of the i-th element. N is the number of elements.

From Eq (6.6), the sensitivity of total strain energy can be derived as :

$$\frac{dU}{dh_i} = [\int_{V_i} (\int f d\overline{\epsilon} - \frac{f^2}{f'}) dV_i] \frac{\partial E_i}{\partial h_i} \tag{6.11}$$

6.3 Numerical results

In this section, a 2-D and a 3-D numerical examples with both geometric and material nonlinearity are presented to demonstrate the application for the proposed method in sensitivity analysis. ANSYS commercial finite element codes for large deformations are used to obtain standard structural analysis results.

To evaluate the accuracy of the new method, numerical results obtained by the proposed method are compared with those from a finite difference derivative, whereas the design sensitivity is expressed as $\Delta U/\Delta h$. For each example, we assume the material modulus is a function of design variables.

$$E_i = E_{i0} g(h) \tag{6.12}$$

where E_{i0} is modulus constant of i-th element,

$$g(h) = h^2 \qquad \text{with} \quad 0 \leq h \leq 1 \tag{6.13}$$

The following three different material behaviors are studied in each example:

Case 1: The softening material modeled by the power-law stress-strain relation,

$$f(\overline{\varepsilon}) = \overline{\varepsilon}^n \qquad \text{with} \quad n < 1. \tag{6.14}$$

The stress-strain behavior is shown in Figure 1.

Case 2: The stiffening material modeled by the power-law stress-strain relation,

$$f(\overline{\varepsilon}) = \overline{\varepsilon}^n \qquad \text{with} \quad n > 1. \tag{6.15}$$

The stress-strain behavior is shown in Figure 2.

Case 3: With typical rubber-like material behavior, the stress-strain relation can be described in the following form of a series expansion

$$f(\overline{\varepsilon}) = \overline{\varepsilon} - 40\overline{\varepsilon}^2 + 625\overline{\varepsilon}^3. \tag{6.16}$$

The stress-strain behavior is shown in Figure 3.

6.3.1 Example 1: two-dimensional plane

A simple two-dimensional plane is considered as a first example to study the application and accuracy of the proposed approach. This example has 5×5 finite elements and

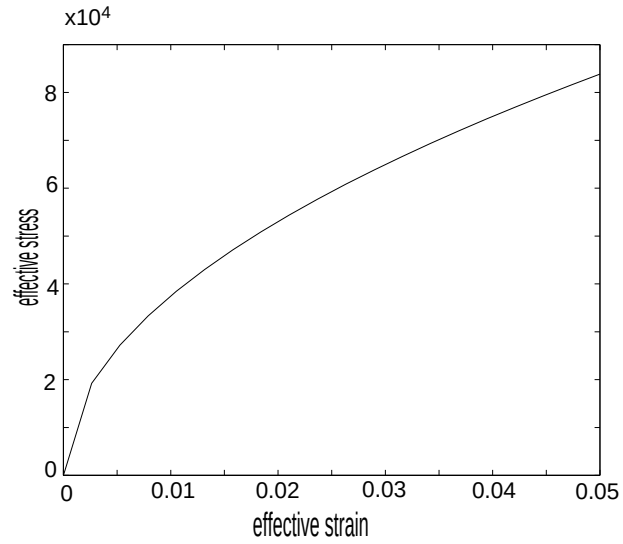

Figure 6.1: The stress-strain behavior: case 1(power law with $n < 1$)

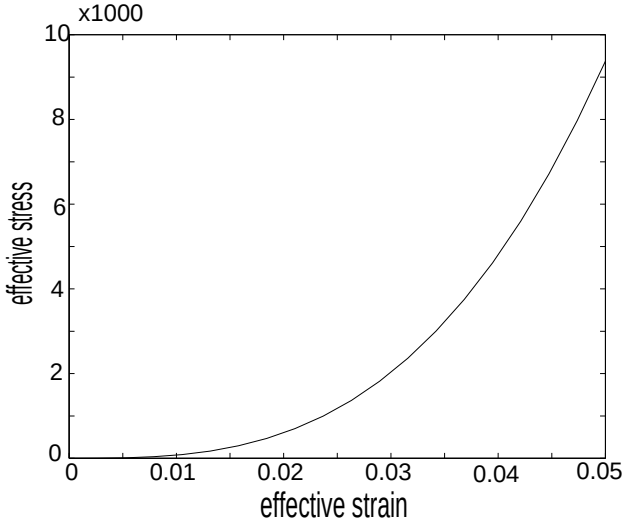

Figure 6.2: The stress-strain behavior: case 2(power law with $n > 1$)

external loads are applied to the free end of beam (Figure 3). The results in Tables 1, 2, and 3 represent the sensitivities of total strain energy of four different elements calculated by the new method and finite difference derivative method, as well as their relative differences for nonlinear material behaviors in cases 1, 2, and 3, respectively. As shown in Tables 1, 2 and 3, sensitivity predictions are in close agreement with finite difference results for three different material behaviors with large deformation.

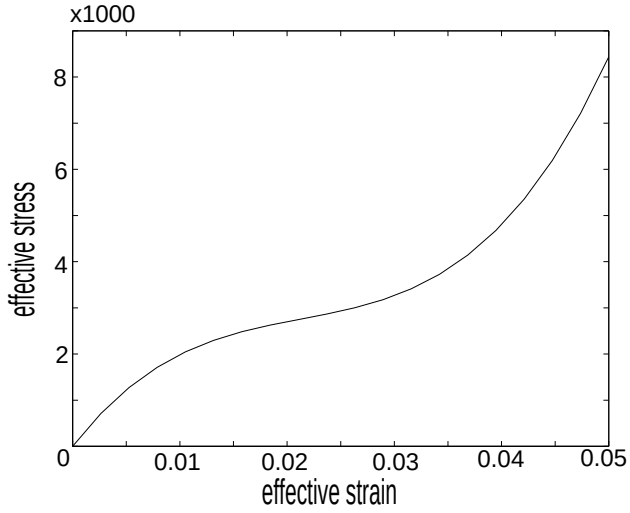

Figure 6.3: The stress-strain behavior: case 3(typical rubber behavior)

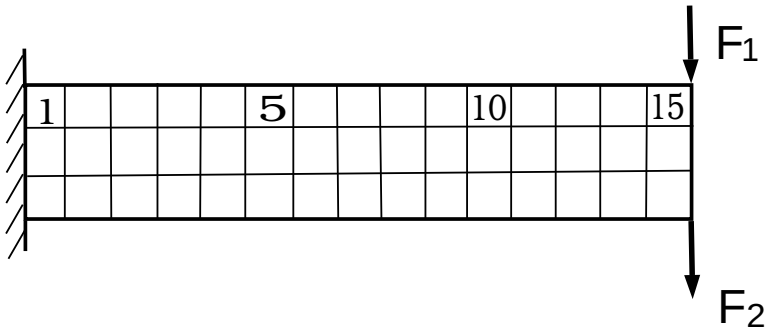

Figure 6.4: Example 1: two dimensional plane

No. of elem	New method	Finite difference derivative	The relative difference
1	-8.4221	-8.3825	0.47%
5	-4.5432	-4.5213	0.48%
10	-5.3244	-5.3015	0.43%
15	-6.8932	-6.8622	0.45%

Table 6.1: **Comparison of the results of plane for case 1**

No. of elem	New method	Finite difference derivative	The relative difference
1	-9.4121	-9.3633	0.55%
5	-5.9747	-6.0171	0.71%
10	-6.2121	-6.2537	0.67%
15	-8.9955	-9.0395	0.49%

Table 6.2: **Comparison of the results of plane for case 2**

No. of elem	New method	Finite difference derivative	The relative difference
1	-9.5431	-9.6299	0.91%
5	-5.7771	-5.8181	0.71%
10	-6.7313	-6.7777	0.69%
15	-7.9991	-8.0694	0.88%

Table 6.3: **Comparison of the results of plane for case 3**

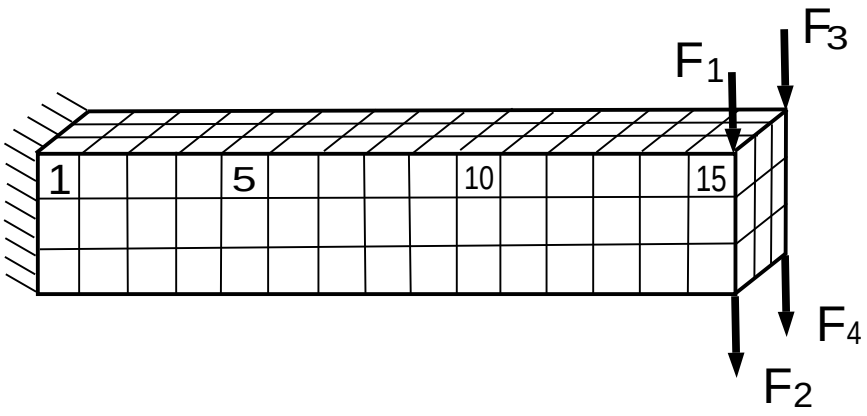

Figure 6.5: Example 2: 3-D solid

6.3.2 Example 2: 3-D solid

The second example presents a 3-D problem with $5 \times 5 \times 5$ finite elements as external loads are applied to the free end of solid(Figure 4).

The results in Tables 4, 5, and 6 represent the sensitivities of four different elements for a 3-D solid obtained by the new method and finite different derivative method, as well as their relative differences for cases 1, 2, and 3 nonlinear material behavior respectively. As shown in Tables 4, 5, and 6, excellent agreement between sensitivity predictions is obtained from proposed method and finite differences are obtained for the three dimensional model.

No. of elem	New method	Finite difference derivative	The relative difference
1	-12.2422	- 12.1871	0.45%
5	-7.2311	- 7.1963	0.48%
10	-9.8843	- 9.8378	0.47%
15	-10.3211	-10.2725	0.44%

Table 6.4: **Comparison of the results of 3-D solid for case 1**

No. of elem	New method	Finite difference derivative	The relative difference
1	-13.3121	-13.4146	0.77%
5	-8.9312	- 9.0124	0.91%
10	-10.6662	-10.7601	0.88%
15	-11.4321	-11.5087	0.67%

Table 6.5: **Comparison of the results of 3-D solid for case 2**

No. of elem	New method	Finite difference derivative	The relative difference
1	-13.3111	- 13.3990	0.66%
5	-8.3211	-8.3818	0.73%
10	-9.9976	-10.0776	0.80%
15	-11.8843	-11.9639	0.67%

Table 6.6: **Comparison of the results of 3-D solid for case 3**

6.4 Conclusion

In this chapter, a generalized "exact" method of sensitivity analysis for strain energy is presented for material nonlinear models with large deformation. The examples show the high incidence of agreement between the results of the proposed method and the results of a finite difference method for different material behaviors with large strain. The analysis applies as well in two and three-dimensional problems.

Chapter 7

Sensitivity Analysis in Structure with Uncertainties

7.1 Introduction

In rather extensive literature on optimal design, major attention is paid to optimization of constructions that are subject to a fixed loading. However, the typical situation for the practical use of an optimal design is different: acting forces are either varying in time, or varying from one sample to another, or are unpredictable. This motivates a reformulation of the problem to account for possible variations and uncertainties in loading.

One can foresee a significant change in the reformulated design if the loading is not completely known. Indeed, the optimality requirement forces the structure to concentrate its resistivity against applied loading, since its abilities to resist other loadings are limited. This high sensitivity to the loading restricts the applicability of most optimal designs.

7.2 Means of general nonlinear function of single random variable

The approximations of the mean deviations of a general nonlinear function of random variables can be obtained by means of the "partial derivative rule". Consider a nonlinear function of a single random variable as

$$Y = g(X) \tag{7.1}$$

Expanding the function in a Taylor's series about the mean value and neglecting terms involving third and higher order derivations yields

$$Y = g(\mu_X) + g'_{\mu_X}(X - \mu_X) + \frac{1}{2}g''_{\mu_X}(X - \mu_X)^2 \tag{7.2}$$

Since $g(\mu_X)$ and g'_{μ_X} are constants, the mean value of Y may be approximated as

$$\mu_Y \quad = \quad E[g(\mu_X) + g'_{\mu_X}(X - \mu_X) + \frac{1}{2}g''_{\mu_X}(X - \mu_X)^2]$$

$$= \quad g(\mu_X) + \frac{1}{2} g''_{\mu_X} \sigma_X^2 \tag{7.3}$$

where μ_X and σ_X^2 are the mean and derivation of variable X

7.3 Uncertain Applied Force and Linear Material

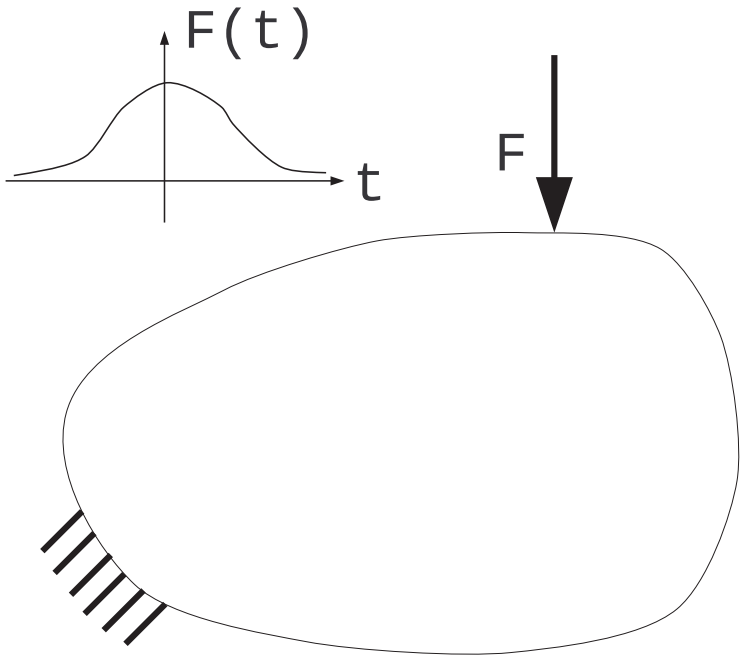

Figure 7.1: Uncertain Magnitude of External Forces

In this case, an object on which external forces are applied with the uncertain magnitude follows a distribution with the mean μ_{F_1} and variation σ_{F_1}. The total strain energy can be expressed as

$$U = F^T [K]^{-1} F \tag{7.4}$$

where $[K]$ is stiffness matrix, U is the total strain energy , and $F = \begin{Bmatrix} F_1 \\ F_2 \\ F_3 \\ F_4 \\ \cdots \\ F_n \end{Bmatrix}$ is the vector of external forces. In order to obtain the mean value of the total strain energy by using the result derived in section 2, we need to get the second derivation of the

strain energy of external force. To simplify the problem, consider that there is only one single uncertain external force F_1. We can get

$$\frac{\partial U}{\partial F1} = 2 \begin{Bmatrix} 1 \\ 0 \\ 0 \\ 0 \\ ... \\ 0 \end{Bmatrix} [K]^{-1} F \tag{7.5}$$

Therefore, we can get

$$\frac{\partial^2 U}{\partial F_1^2} = 2 \begin{Bmatrix} 1 \\ 0 \\ 0 \\ 0 \\ ... \\ 0 \end{Bmatrix} [K]^{-1} \{1, 0, 0, 0, ..., 0\} \tag{7.6}$$

The result in fact gives the strain energy with unit external force. Therefore, according to the result in section 1, the mean value of total strain energy can be expressed as:

$$\mu_U = U(\mu_{F1}) + U(F_1^0)\sigma_{F_1}^2 \tag{7.7}$$

where $U(\mu_{F1})$ is the strain energy calculated with the mean value of F_1, and $U(F_1^0)$ is the strain energy calculated with unit force of F_1. For linear material, it is well-known that:

$$\frac{dU}{dh} = -\frac{\partial U}{\partial h}|_{fix-strain} \tag{7.8}$$

where U is the strain energy and h is the design variable. So, the sensitivity of the mean value of strain energy can be easily derived as:

$$\frac{d\mu_U}{dh} = -\frac{\partial U}{\partial h}|_{fix-strain}(\mu_{F1}) - \frac{\partial U}{\partial h}|_{fix-strain}(F_1^0)\sigma_{F_1} \tag{7.9}$$

7.4 Uncertain Young's Modulus for Non-linear Structures

Consider nonlinear structures as represented by effective strain and effective stress as

$$\overline{\sigma} = Ef(\overline{\varepsilon}) \tag{7.10}$$

In this case, the modulus E is a uncertain variable. The strain energy density can thus be written as

$$u = E(h) \int f(\overline{\varepsilon}) d\overline{\varepsilon} \tag{7.11}$$

For previous derivation of sensitivity analysis for non-linear structure, we already got

$$\frac{\partial \overline{\varepsilon}}{\partial E} = -\frac{1}{E} \frac{f(\overline{\varepsilon})}{f'(\overline{\varepsilon})} \tag{7.12}$$

In order to get the mean value of strain energy density represented by the mean value and variation of the modulus E, we need to obtain the second order derivative of strain energy by the modulus E. Since the strain energy density can be expressed as:

$$u = E \int f(\overline{\varepsilon}) d\overline{\varepsilon} \tag{7.13}$$

we can obtain

$$\frac{du}{dE} = \int f(\overline{\varepsilon}) d\overline{\varepsilon} + E f(\overline{\varepsilon}) \frac{\partial \overline{\varepsilon}}{\partial E} \tag{7.14}$$

By substituting the result of Eq (7.12) into Eq (7.14), we have

$$\frac{du}{dE} = \int f(\overline{\varepsilon}) d\overline{\varepsilon} - \frac{f^2(\overline{\varepsilon})}{f'(\overline{\varepsilon})} \tag{7.15}$$

Taking the second derivative by the modulus E, we get

$$\begin{aligned} \frac{d^2u}{dE^2} &= [f(\overline{\varepsilon}) - \frac{2f(\overline{\varepsilon})f'(\overline{\varepsilon}) - f^2(\overline{\varepsilon})f''(\overline{\varepsilon})}{[f'(\overline{\varepsilon})]^2}] \frac{\partial \overline{\varepsilon}}{\partial E} \\ &= -\frac{f^2(\overline{\varepsilon})[f'(\overline{\varepsilon})]^2 - 2f^2(\overline{\varepsilon})f'(\overline{\varepsilon}) + f(\overline{\varepsilon})f'(\overline{\varepsilon})f''(\overline{\varepsilon})}{E[f'(\overline{\varepsilon})]^3} \end{aligned} \tag{7.16}$$

Therefore, according to the result in section 1, the mean value of total strain energy can be expressed as:

$$\mu_U = U(\mu_E) + \frac{d^2U}{dE^2}(\mu_E)\sigma_E^2 \tag{7.17}$$

Since this expression is the explicit form of the modulus E, it is straight-forward to obtain the sensitivity of the mean of strain energy by taking the derivative of E.

Especially for linear material, we have

$$f(\overline{\varepsilon}) = \overline{\varepsilon} \tag{7.18}$$

The result of Eq (7.16) can be reduced to

$$\frac{d^2U}{dE^2} = -\frac{\overline{\varepsilon}^2}{2} \tag{7.19}$$

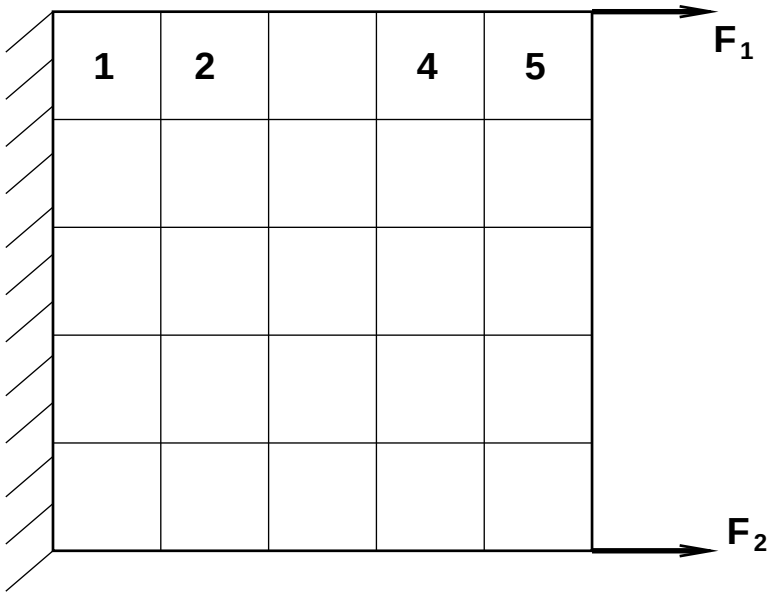

Figure 7.2: Example 1: two dimensional plane

7.5 Numerical results for Uncertain Applied Force with Linear Material

In this section, a 2-D example is presented to demonstrate the application for the proposed method in sensitivity analysis. The Monte Carlo simulation is used to verify the results from the analytical results .

7.5.1 Example: two-dimensional plane

A simple two-dimensional plane is considered as an example to study the application and accuracy of the proposed approach. This example has 5×5 finite elements and external loads are applied to the free end of beam (Figure 3). The results in Tables 7.1 represent the sensitivities of total strain energy of four different elements calculated by the analytical method and Monte Carlo simulation, as well as their relative differences. As shown in Tables 1, 2 and 3, sensitivity predictions are in close agreement with Monte Carlo results.

7.6 Numerical results for Uncertain Young's Modulus with Non-linear Materials

In this section, a 2-D and 3-D numerical example with both geometric and material nonlinearity are presented to demonstrate the application for the proposed method in

No. of elem	New method	Monte Carlo Simulation	The relative difference
1	-32.3112	-32.5697	0.8%
2	-25.4232	-25.6266	0.56%
4	-28.3452	-28.5720	0.91%
5	-20.1111	-20.2720	0.78%

Table 7.1: **Comparison of the results of plane**

sensitivity analysis. The Monte Carlo simulation is used to verify the results from the analytical results .

For each example, we assume the material modulus is a function of design variables.

$$E_i = E_{i0} g(h) \tag{7.20}$$

where E_{i0} is the modulus constant of i-th element,

$$g(h) = h^2 \qquad \text{with} \;\; 0 \leq h \leq 1 \tag{7.21}$$

The following three different material behaviors are studied for each example.

Case 1: The softening material modeled by the power-law stress-strain relation,

$$f(\bar{\varepsilon}) = \bar{\varepsilon}^n \qquad \text{with} \;\; n < 1. \tag{7.22}$$

The stress-strain behavior is shown in Figure 1.

Case 2: The stiffening material modeled by the power-law stress-strain relation,

$$f(\bar{\varepsilon}) = \bar{\varepsilon}^n \qquad \text{with} \;\; n > 1. \tag{7.23}$$

The stress-strain behavior is shown in Figure 2.

Case 3: With typical rubber-like material behavior, the stress-strain relation can be described in the following form of a series expansion

$$f(\bar{\varepsilon}) = \bar{\varepsilon} - 40\bar{\varepsilon}^2 + 625\bar{\varepsilon}^3. \tag{7.24}$$

The stress-strain behavior is shown in Figure 3.

7.6.1 Example 1: two-dimensional plane

A simple two-dimensional plane is considered as a first example to study the application and accuracy of the proposed approach. This example has 5×5 finite elements and

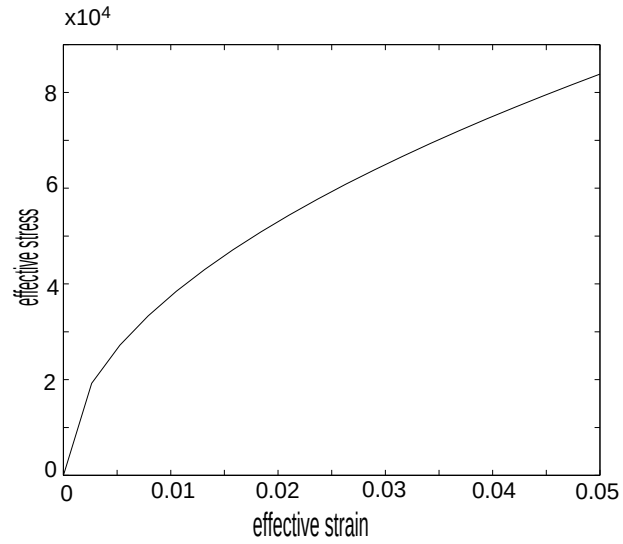

Figure 7.3: The stress-strain behavior: case 1(power law with $n < 1$)

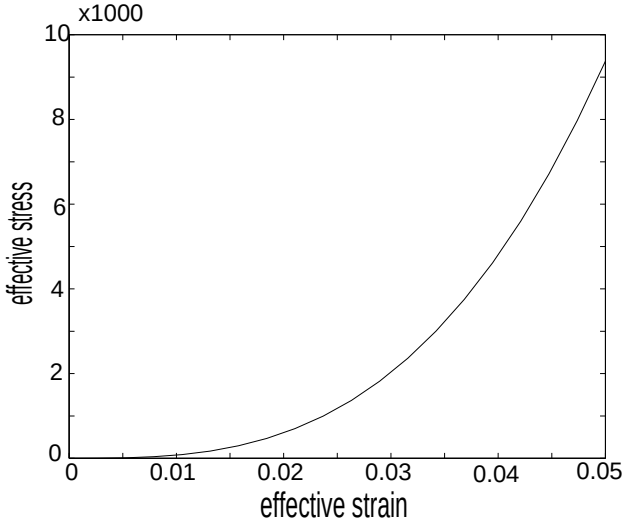

Figure 7.4: The stress-strain behavior: case 2(power law with $n > 1$)

external loads are applied to the free end of beam (Figure 3). The external force is applied with the uncertain magnitude following a distribution. The results in Tables 1, 2, and 3 represent the sensitivities of total strain energy of four different elements calculated by the new method and Monte Carlo simulation, as well as their relative differences for nonlinear material behaviors in cases 1, 2, and 3, respectively. As shown in Tables 1, 2 and 3, sensitivity predictions are in close agreement with the results derived by a Monte Carlo simulation.

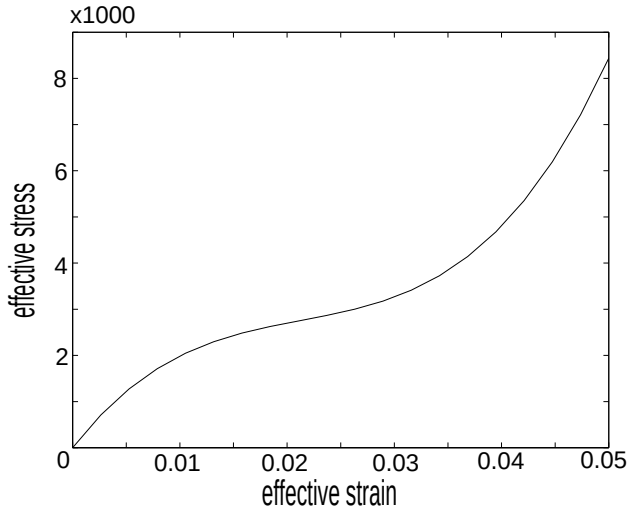

Figure 7.5: The stress-strain behavior: case 3(typical rubber behavior)

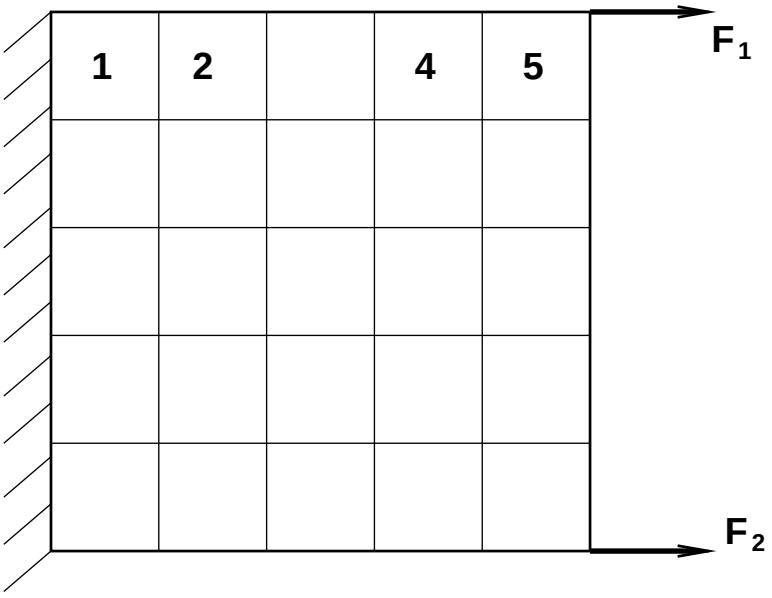

Figure 7.6: Example 1: two dimensional plane

No. of elem	New method	Monte Carlo Simulation	The relative difference
1	-8.4221	-8.3825	0.47%
2	-4.5432	-4.5213	0.48%
4	-5.3244	-5.3015	0.43%
5	-6.8932	-6.8622	0.45%

Table 7.2: **Comparison of the results of plane for case 1**

No. of elem	New method	Monte Carlo Simulation	The relative difference
1	-9.4111	-9.3631	0.51%
2	-5.3133	-5.2671	0.87%
4	-6.9881	-6.9343	0.77%
5	-7.3121	-7.2470	0.89%

Table 7.3: **Comparison of the results of plane for case 2**

No. of elem	New method	Monte Carlo Simulation	The relative difference
1	-10.8777	-10.7787	0.91%
2	-5.0991	-5.0491	0.98%
4	-7.0011	-6.9339	0.96%
5	-8.9121	-8.8345	0.87%

Table 7.4: **Comparison of the results of plane for case 3**

7.6.2 Example 2: 3-D solid

The second example presents a 3-D problem with $5 \times 5 \times 5$ finite elements as external loads are applied to the free end of the solid(Figure 4). In the example, Yong's Modulus is an uncertain variable following a distribution.

The results in Tables 4, 5, and 6 represent the sensitivities of four different elements for a 3-D solid obtained by the new method and Monte Carlo simulation, as well as their relative differences. As shown in Tables 4,5 and 6, excellent agreement between sensitivity prediction obtained from the proposed method and Monte Carlo method is obtained for the three dimensional model.

No. of elem	New method	Monte Carlo Simulation	The relative difference
1	-12.2422	-12.1871	0.45%
2	-7.2311	-7.1963	0.48%
4	-9.8843	-9.8378	0.47%
5	-10.3211	-10.2725	0.44%

Table 7.5: **Comparison of the results of 3-D solid for case 1**

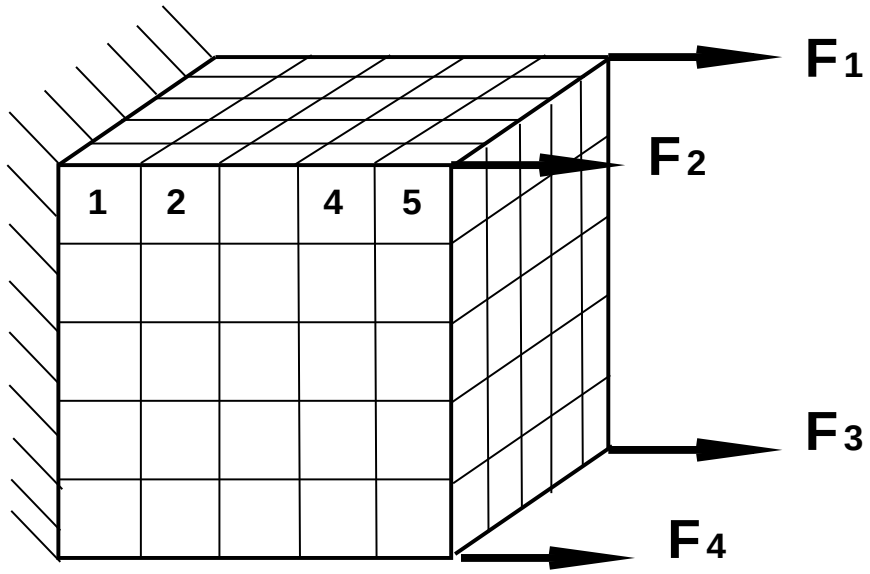

Figure 7.7: Example 2: 3-D solid

No. of elem	New method	Monte Carlo Simulation	The relative difference
1	-14.1211	-14.0279	0.66%
2	-8.4321	-8.3494	0.98%
4	-10.3311	-10.2412	0.87%
5	-13.2122	-13.0973	0.87%

Table 7.6: **Comparison of the results of 3-D solid for case 2**

No. of elem	New method	Monte Carlo Simulation	The relative difference
1	-15.3111	-15.1672	0.94%
2	-8.5432	-8.4774	0.77%
4	-11.3433	-11.2466	0.87%
5	-13.1211	-12.9964	0.95%

Table 7.7: **Comparison of the results of 3-D solid for case 3**

7.7 Conclusion

In this chapter, a generalized "exact" method of sensitivity analysis for strain energy is presented for problems with uncertain variables . The term "generalized" is used for defining the method because it may be applied to nonlinear elastic structures with an arbitrary relation between stress and strain and large deformation with small strains. The method is "exact" and computationally efficient because it is a closed-form solution. The examples demonstrate the high incidence of agreement between the results of the proposed method and the results of Monte Carlo method for both uncertain external forces and uncertain Young's Modulus. The analysis applies as well in two and three-dimensional problems.

Chapter 8

CONCLUSIONS AND FUTURE WORK

8.1 Conclusions

In the dissertation, sensitivity analysis of total strain energy for nonlinear structures is studied. Based on the law of energy-consistent, the effective strain and stress have been defined to provide scalar measures of the strain and stress for the two and three dimensional problems. The total strain energy is transformed in the form of the effective stain and stress. A closed-form approach for sensitivity calculation is derived which can be generalized used for different material behaviors.

The effective model is extended to large deformation problems using the 2nd Piola-Kirchhoff stress and Green-Langrange stress. The similar derivation of sensitivity anaylysis for nonlinear material is used to derive a closed-form solution of sensitivity analysis for large deformation

The numerical examples with both geometric and material nonlinearity are presented to demonstrate the applications for the proposed sensitivity analysis calculation for strain energy. To evaluate the accuracy of the new method, numerical results obtained by the proposed method are compared with those from both analytical solution (for simple geometry) and from finite differencing method. The case studies are performed for different material behaviors: strain softening material; strain stiffing material and rubber-like material along with large deformation. The numerical results for both two dimensional plate and three dimensional solid have been presented.

The closed-form solution of design sensitivity is also applied for reliability-based structural design. Specifically, the case studies are performed for the problem for the uncertain applied force performed, and uncertain Young's modulus with nonlinear materials. The numerical results obtained by the close-formed solution are compared with those from Monte Carlo simulation.

The numerical examples from different kind of problems have demonstrated a high

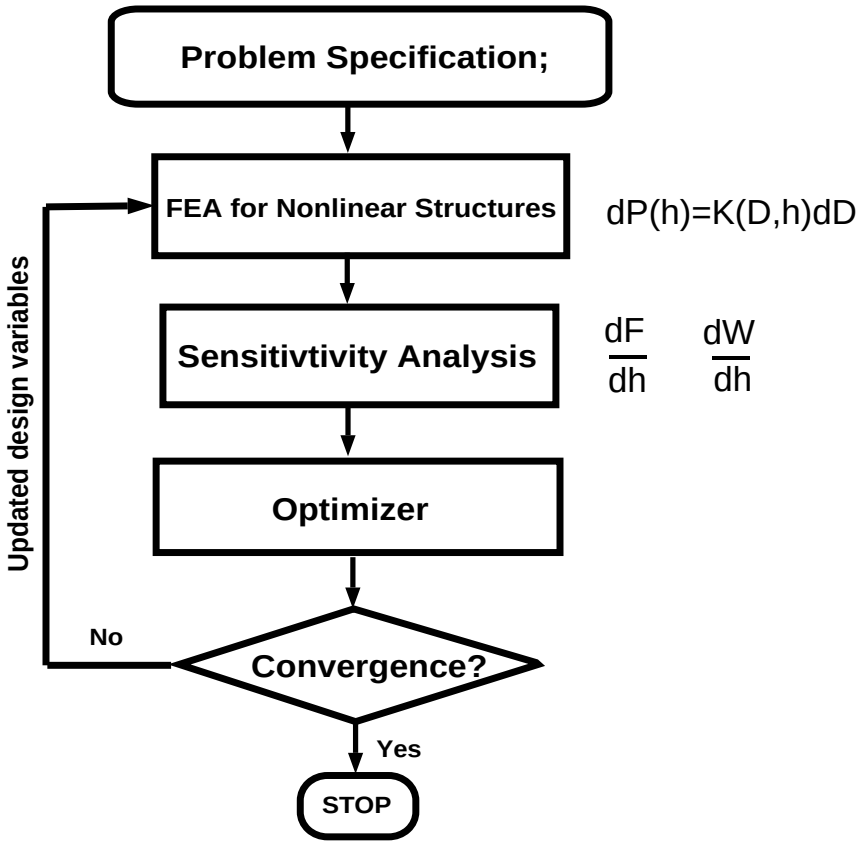

Figure 8.1: Algorithm of Optimization

incidence of agreement between the results from the proposed method and those from the finite difference method.

8.2 Future Research Directions

To develop an optimal design process for nonlinear structures, it is necessary to develop methods of design sensitivity analysis for nonlinear response. The methods should be efficient, stable and reliable for general applications. The methods are usually related to structural analysis procedures. Some nonlinear structural analysis methods may not be suitable in the overall structural design optimization process. Therefore, development of design design sensitivity analysis and hence the optimal design process for nonlinear system is possible through a thorough understanding of the nonlinear structural analysis procedures.

Design sensitivity analysis in this study has provided design derivatives that constitute a major task for different kinds of structural optimization algorithm. These

derivatives are also important in their own right as they represent trend for the structural performance functions. The future study should more focus on the application of optimization for different problems that were addressed in the study. The Figure 8.1 give the general algorithm of optimization for nonlinear problems. The sensitivity calculation is equivalent to the mathematical problem of obtaining the derivatives of the solutions of those equation with respect to the design variables. Compared with the traditional approaches of sensitivity analysis, i.e., the finite difference method, the adjoint variable method or the direct differentiation method, the proposed closed form solution will greatly reduce the calculation, and will be easily implemented.

References

[1] Shinji Nishwaki, Seungjae Min and Noboru Kikuchi. Structural Optimization Based on Flexibility and Its Appliction to Design of Automobiles. *Design Optimization with Applications in Industry (Ed. by R.-J. Yan and D.E. Smith)*, 1997, AMD-227, 1-11.

[2] E.J. Haug, K.K. Choi and V. Komkov, *Design Sensitivity Analysis of Structural System* (Academic Press. New York, 1996)

[3] H.M Adelman and R.T. Haftka. *Sensitivity Analysis for Discret Structural System.* AIAA J. 24 (1986) 823-832.

[4] D.A. Tortorelli and R.B. Haber. First-order Disign Sensitivities for Transient Conduction Problems by an Adjoint Method. *Internat. J. Number. Methods Engrg.*, 28, 733-752, 1989.

[5] Y.S. Ryu. M. Haririan, C.C. Wu and J.S. Arora. Structural Design Sensitivity Analysis of Nonlinear Response. *Comput. Structues*, 21, 245-255, 1985.

[6] J.J. Tsay and J.S. Arora, Nonlinear Stuctural Design Sensitivities Analysis for Path Dependent Problems. Part 1: General Theory. *Comput. Methods Appl. Mech. Engrg.*, 81,183-208, 1990.

[7] C.C. Wu and J.S Arora. Design Sensitivity Analysis and Optimization of Nonlinear Structural Response Using Incremental Procedure. *AIAA J*, 25, 1118-1125, 1987.

[8] J.J. Tsay, J.E.B. Cardoso and J.S. Arora. Nonlinear Structural Design Sensivity Analysis for Path Depedent Problems. Part 2: Analytical Examples. *Comput. Methods Appl. Mech. Engrg.*, 81, 209-228, 1990.

[9] S. Mukherjee and A. Chandra. A Bundary Element Formulation for Design Sensitivity in Materially Nonlinear Problems. *Acta Mech*, 78, 143-253, 1989.

[10] Q. Zhang and S. Mukherjee. Design Sensitivity Coefficients for Elastic-viscoplastic Problems by Boundary Element Methods. *Internat. J. Number. Methods Engrg.*, 34, 947-966, 1992.

[11] R.B. Haber, D.A. Tortorelli, C.A. Vidal and D.G. Phelan. Design Sensitivity Analysis of Nonlinear Structues-I: Large-deformation Hyperelasticity and History-dependent Material Response, in: M.P. Kamat. ed.. *Structual Optimization: Status Promise. AIAA Progess in Astronautics and Aeronauties Series(AIAA, New York)*, 369-405, 1993.

[12] C.A. Vidal, H.-S. Lee and R.B. Haber. The consistent Tangent Operators for Design Sensitivity Analysis of History-depedent Response. *Comput. Systems Engrg.*, 2, 1561-1576, 1985.

[13] C.A. Vidal. A Consistent Design Sensitivity Analysis Formulation for Systems with History-dependent Response. *Ph.D Thesis, Department of Civil Engineering, Universiy Illinois, Urbana-Champaign, IL*, 1992.

[14] H. Chickermane and H.C. Gea. A New Local Function Approximation Method for Structural Optimization Problems. *International Journal for Numerical Methods in Engineering*, 39:829–846, 1996.

[15] H.C. Gea. Topology Optimization: A New Micro-Structure Based Design Domain Method. *Computers and Structures*, 61(5):781-788, 1996.

[16] E.J. Haug and J. Cea. *Optimization of Distributed Parameter Structures, Vols. I and II.* Sijthoff and Noordhoff, 1981.

[17] J.H. Luo and H.C. Gea. Modal Sensitivity Analysis of Coupled Acoustic-Structural Systems. *Journal of Vibration and Acoustic*, 1997.

[18] Z.D. Ma, N. Kikuchi and I. Hagiwara. Structural Topology and Shape Optimization for a Frequency Response Problem. *Computational Mechanics*, 13:157-174, 1993.

[19] K. Suzuki and N. Kikuchi. A Homogenization Method for Shape and Topology Optimization. *Computer Methods in Applied Mechanics and Engineering*, 93:291-318, 1991.

[20] Bathe,Klaus-Jurgen. Finite Element Procedures. Prentice-Hall, Inc., 1996.

[21] Zienkiewicz, O. C. and Taylor, R. L. The Finite Element Method. Volume 2, McGraw-Hill, UK, 1996.

[22] Stoker, J. J. Nonlinear Elasticity. the Saint Catherine Press, Ltd., Tempelhof, Brugge, 1968.

[23] Hinton, E., Owen, D. R. J. and Taylor, C. Recent Advances in Non-linear Computational Mechanics. Pineridge Press Limited, Swansea, UK, 1982.

[24] Hibbitt, H. D., Marcal, P. V. and Rice, J. R.. A finite element formulation for problems of large strain and large displacement. *Int. J. Solids Structures*, pp. 1069-1086, 1970.

[25] Gengdong Cheng. Introduction to structural optimization. *Solid Mechanics*, 1993

[26] J.L.T.Santos and K.K.Choi,P.. Shape design sensitivity analysis of nonlinear structural systems. *Structural Optimization*, Vol.4,23-35, 1992

[27] J.H.Lou and H.C.Gea,P.. Optimal Orientation of Orthotropic Materials Using an Energy Method. *Structural Optimization*, 1997.

[28] R.T. Haftka. On the accuracy of shape sensitivity. *Structural Optimization*, Vol.3,1-6 . pp.34-43, 1991.

[29] K.E. Bisshopp and D.C. Drucker. Large deflection of cantilever beams. *Q. Appl. Math.*,3, 272, 1945.

[30] R. Frisch-Fay, 1962, *Flexible Bars*,Butterworth, Washington, D.C., 1962.

[31] W. Gorski, 1976. A review of literature and a bibliography on finite elastic deflections of bars. *Trans. Inst. Engnrs Australia Civ. Engng Trans.*, 18, 74, 1976.

[32] K. Mattiasson. Numerical Results from Large Deflection Beam and Frame Problem Analyzed by Means of Elliptic Integrals. *International Journal for Numerical Methods in Engineering*,Vol.17,145, 1981.

[33] L.L. Howell and James N. leonard. Optimal Loading Conditions for Nonlinear Deflections. *Int. Journal Non-linear Mechanics*, Vol.32,505, 1988.

[34] Y.S. Ryu, M. Haririan, C.C. Wu and J.S. Arora. Structural Design Sensitivity Analysis of Nonlinear Response. *Computers and Structures*, 21, 1/2, 245, 1985.

[35] J.S. Arora and J. E. B. Cardoso. Nonlinear Structural Design Analysis for Path Dependent Problems. Part 1: General Theory. *Computer Methods in Applied Mechanics and Engineering*, 81, 183, 1990.

[36] J.J. Tsay, J. E. B. Cardoso and J.S. Arora. Nonlinear Structural Design Analysis for Path Dependent Problems. Part 2: Analytical Examples. *Computer Methods in Applied Mechanics and Engineering*, 81, 209, 1990.

[37] Kyung K. Choi and Jose L. T. Santos. Design Sensitivity Analysis of Non-linear Structural Systems Part 1: Theory. *International Journal for Numerical Methods in Engineering*, 24, 2039, 1987.

[38] Jose L. T. Santos and Kyung K. Choi. Shape Design Sensitivity Analysis of Non-linear Structural Systems. *Structural Optimizations*, 4, 23, 1992.

[39] Freundenthal, A. M, Gerrelts, J. M. and Shinozuka, M.. The Analysis of Structural Safety. *Journal of the Structural Division*, ASME, Vol. 92. No. ST1, Proc. Paper 4682, Feb., 1966. pp.267-325, 1966.

[40] Moses, F.. Sensitivity Studies in Structural Reliability, 1970.

[41] Mischke, C. R., 1987. Prediction of Stochastic Endurance Strength. *Journal of vibration, Acoustic, Stress, and Reliability in Design*, ASME, Vol. 109. pp.113-122, 1987.

[42] Moses, F.. Sensitivity Studies in Structural Reliability. *Structural Reliability and Codified Design*, N. C. Lind, Ed., Solid Mechanics Division, University of Waterloo, Study No. 2, pp. 1-17, 1970.

[43] Frangopol, D. M.. Sensitivity of Reliability-Based Structural Optimization. *Journal of Structural Engineering*,ASME, Vol. 111, No. 8, Aug., pp. 1703-1721, 1985.

[44] Frangopol, D. M.. Towards Reliability-Based Computer-Aided Optimization of Reinforced Concrete Structures. *Engineering Optimization*, Vol. 18, No. 4, pp. 301-313, 1985.

[45] Chang, K. H.; Yuy, X.; Choi, K.K.. Shape design sensitivity analysis and optimization for structural durability. *Int. J. Num. Mech. Eng.*, 1997.

[46] Rao, B.. *Reliability-Based Design,* McGraw-Hill, Inc., New York, 1992.

[47] Pedersen, P. Some general optimal design results using anisotropic. power law nonlinear elasticity. *Structural Optimization*, Vol. 15. pp.73-80, 1998.

[48] Howell, L.L.; Rao, S. S.. Reliability-Based Optimal Design of a Bistable Compliant Mechanism. *Journal of Mechanical Design*, Vol. 116. pp.1115-1121, 1994.

[49] C.Y. Sheu and W. Prager. Optimal Plastic Design of circular and annual sandwich plates wiht piecewise constant cross-section. *J. Mech Phys. Solids*, Vol. 17. pp.11-16, 1969.

[50] I. Kaneko and G Maier. Optimal Design of Plastic Structures Under Displacement Constraints. *Comput. Methods Appl. Mech. Eng.*, Vol. 27. pp.369-391, 1981.

[51] M.P. Bendoe and J. Sokolowski. Sensitivity analysis and optimization of elastic-plastic structurs. *Eng. Optim.*, Vol. 11. pp.31-38, 1987.

[52] M.P. Bendoe and J. Sokolowski. Design sensitivity analysis of elastic-plastic analysis problem. *Mech. Struct.*, Vol. 16. pp.81-102, 1988.

[53] D. Ray, K.S. Pister and E. Polak. Sensitivity analysis for hysteretic dynamic systems: theory and applications. *Comput. Methods Appl. Mech. Eng.*, Vol. 14. pp.179-208, 1978.

[54] J.J. Tsay and J.S. Arora. Design sensitivity analysis of nonlinear structures with history dependent effects. *Technical Report Optimal Design Laboratory, The University of Iowa*, ODL88,4. 1988.

[55] J.J. Tsay and J.S. Arora. Nonlinear structural design sensitivity analysis for path dependent problem, Part 1: general theory. *Comput. Methods Appl. Mech. Eng.*, Vol 81. pp.183-228. 1990.

[56] J.J. Tsay, J.E.B. Cardoso and J.S. Arora. Nonlinear structural design sensitivity analysis for path dependent problem, Part 2: analytical examples. *Comput. Methods Appl. Mech. Eng.*, Vol 81. pp.183-228. 1990.

[57] J.J. Tsay and J.S. Arora. Optimal Design of nonlinear structures with path depedent response. *Struc. Optim..*, Vol 1. pp.243-253. 1989.

[58] J.S. Arora and T.H. Lee. Design sensitivity analysis of nonlinear structures III: shape variation of viscoplastic structures. *Structural Optimization: Status and Promise. AIAA Series: Progress in Astronautics and Aeronautis*, Ch 17 1993.

[59] P. Martinez, P. Marti and O.M. Querin. Growth method for size, topology, and geometry optimization of truss structures. *Struct Multidisc Optim*, 33: 13-26, 2007

[60] Jimmy Forsberg and Larsgunnar Nilsson. Topology optimization in crashworthiness design. *Structural Multidisc Optimization*, 33: 1-12, 2007

[61] G Kharmanda, N. Olhoff and A. El-Hami. Optimum values of structural safety factors for a predefined reliability level with extension to multiple limit states. *Structural Multidisc Optimization*, 27: 421-434, 2004

[62] J.S Arora and Q. Wang. Review of formulations for structural and mechanical system optimization. *Structural Multidisc Optimization*, 30: 251-272, 2005

[63] Katsuya Mogami, Shinji Nishiwaki and Kazuhiro Izui. Reliability-based structrual optimization of frame structures for multiple failure criteria using topology optimization techniques. *Structural Multidisc Optimization*, 32: 299-311, 2006

[64] Y. Tsompanakis and M. Papadrakakis. Large-scale reliability-based structural optimization. *Structural Multidisc Optimization*, 26: 429-440, 2004

Vita

Qiang Kong

1981-85 B.S., Department of Mechanical Engineering, Hangzhou Institute of Electronic Engineering, Zhejiang, P. R. China.

1987-90 M.S., Department of Mechanical Engineering, Harbin Institute of Engineering, Harbin, P. R. China.

1996-97 Teaching Assitang, Department of Mechanical and Aerospace Engineering, Rutgers, The State University of New Jersey, New Brunswick, New Jersey.

1997-1999 Graduate Assistant, Department of Mechanical and Aerospace Engineering, Rutgers, The State University of New Jersey, New Brunswick, New Jersey.

2007 Ph.D., Department of Mechanical and Aerospace Engineering, Rutgers, The State University of New Jersey, New Brunswick, New Jersey.